Elsevier Editorial System(tm) for NeuroImage
Manuscript Draft

Manuscript Number: NIMG-10-1885R2

Title: Intermittent spike-wave dynamics in a heterogeneous, spatially extended neural mass model

Article Type: Regular Article

Section/Category: Methods & Modelling

Corresponding Author: Mr Marc Goodfellow,

Corresponding Author's Institution: The University of Manchester

First Author: Marc Goodfellow

Order of Authors: Marc Goodfellow; Kaspar Schindler; Gerold Baier

Abstract: Generalised epileptic seizures are frequently accompanied by sudden reversible transitions from low amplitude irregular background activity to high amplitude, regular spike-wave discharges (SWD) in the EEG. The underlying mechanisms responsible for SWD generation and for the apparently spontaneous transitions to SWD and back again are still not fully understood. Specifically, the role of spatial cortico-cortical interactions in ictogenesis is not well studied.

We present a macroscopic, neural mass model of a cortical column which includes two distinct time scales of inhibition. This model can produce both an oscillatory background and a pathological SWD rhythm. We demonstrate that coupling two of these cortical columns can lead to a bistability between out-of-phase, low amplitude background dynamics and in-phase, high amplitude SWD activity. Stimuli can cause state-dependent transitions from background into SWD. In an extended local area of cortex, spatial heterogeneities in a model parameter can lead to spontaneous reversible transitions from a desynchronised background to synchronous SWD due to intermittency. The deterministic model is therefore capable of producing absence seizure-like events without any time dependent adjustment of model parameters.

The emergence of such mechanisms due to spatial coupling demonstrates the importance of spatial interactions in modelling ictal dynamics, and in the study of ictogenesis.

1. Cover Letter

Marc Goodfellow

Manchester Interdisciplinary Biocentre,
The University of Manchester, Manchester M1 7DN, UK.
Phone: +44 (0) 161 3065124,
fax: +44 (0)161 3064556,
email: marc.goodfellow@postgrad.manchester.ac.uk

15th December 2010

NeuroImage

Re: Re-submission of manuscript: Ms. No.: NIMG-10-1885

Dear Editor,

I am writing to re-submit our manuscript entitled “Intermittent spike-wave dynamics in a heterogeneous, spatially extended neural mass model” by Marc Goodfellow, Kaspar Schindler and Gerold Baier.

We would like once again to thank both reviewers for their constructive criticism. We feel this has enabled us to significantly improve the manuscript. We have addressed all concerns and comments by the two reviewers, which are summarized in our file “ResponseToReviewers”.

With best wishes,

Marc Goodfellow

***2. Response to Reviews**

Reviewer #1: The authors have substantially improved the paper, though I still have some residual comments:

1. My main concern is that the evidence for the reported power law in Fig. 9(c) is still a bit weak. By eye it looks like a log-normal distribution (for example) could fit the data at least as well. A more formal procedure for parameter estimation and determining whether a power law really is the best description would be much more compelling (the authors may find this reference helpful: http://arxiv.org/pdf/0706.1062). The distribution should also be sampled with more points and possibly for longer times to reduce sampling errors.

Following the reviewers suggestion we calculated longer time series and studied distributions of more than 1000 seizures. In the new log-log plot (Fig 9c in the revised MS), with the higher resolution obtained, a deviation from the power law assumption can now be seen and is commented on in the text. The testing procedure recommended by the reviewer found the power law assumption was rejected.

In the results section of our revised MS we comment on the deviation from power scaling in the distribution seen in Fig. 9c. This is then discussed in the context of previous publications on the topic. Specifically, we stress that according to theory, the distribution must be expected to change depending upon the parameter values chosen (Chate and Manneville 1987, referenced in the text) and strict power law behaviour is only expected near the onset of intermittency. The example intermittent solution shown in Fig. 9 provides a useful demonstration that such behaviour can be obtained in the model and is a major finding.
However, a complete understanding and characterisation of intermittency in our model requires a thorough study of distributions and scaling with respect to the high dimensional parameter space. This is beyond the scope of the present paper, which focuses on the role of spatial cortico-cortical interactions in ictogenesis. We also reference to the inconsistency in previous experimental findings regarding expected distributions of seizure and non-seizure periods. These points are commented on in the discussion.

2. In Fig. 9(d) the second return map is plotted for the values of the maxima within the laminar phases, whereas Velazquez et al. used the first return map of the lengths of the laminar phases. Is one method preferable to the other?

To test for on-off intermittency and distinguish it from type III intermittency, the second return map of maxima was used in Hramov et. al. 2006, with reference to a previous study also examining time series maxima (Dubios et. al. 193 Physics Review Letters Volume 51 p1446: Experimental evidence of intermittencies associated with a subharmonic bifurcation). We therefore believe this is an appropriate method.

3. The bifurcation diagrams have been greatly improved, though I still feel that Fig. 8 could be better resolved. The sampling of the pBckg region is still a bit coarse; perhaps smaller markers (even just dots?) and extraction of extrema from a longer time series would better show the actual shape of the attractor, which at present looks more like numerical artifact.

The attractor in the pBckg region displays periodic amplitude modulation of all compartments, and thus its shape is adequately represented by the extrema as plotted in the figure. Extraction of extrema from a longer time series would result in an identical picture, as the time varying extrema during the amplitude modulated periods would still be captured. Sampling from shorter periods in between these periods of amplitude modulation would result in a "cleaner" picture, but would not be fully representative of the amplitude modulated dynamics. In the revised MS we more carefully explain this point by introducing the following sentence:
"We stress that although this region with periodic amplitude modulation may look like a noise artifact, it is actually representative of certain periods during the time course in which the amplitude in all compartments undergoes a smooth increase and decrease."

For quasi-periodic dynamics, plotting with small dots would simply produce a short vertical line. As such, no relevant structure is missing from our representation. It is our wish here to maintain consistency with the legend given in Figure 3 and subsequent bifurcation plots, and we therefore opt to keep the markers as they are in this figure.

4. The new definition of phase difference is much better. Just to clarify, in Fig. 8(b) where the Bckg solution has mean phase difference ~pi, are the 300 pairs of phase differences uniformly distributed in [0 2pi)? Or does clustering occur? Also, the 'outlying SWD stars' could probably be wrapped through 2pi so that the solution branches remain continuous; the gray curves could possibly also be shifted similarly.

In the case mentioned by the reviewer, we note that some clustering occurs at 0, pi and 2pi. In accordance with the reviewer's suggestion, the outlying stars have been wrapped through 2pi in Figures 6 and 8. We retain the position of the grey curves in Figure 6 as this facilitates the arrangement of insets in the figure and provides equivalent information to the reviewer's suggestion.

5. I notice that many of the physical quantities are actually dimensional and have units (e.g., it appears that y_0 is in mV, and I and b_f are in s^-1), so they should always be labeled as such in plots and when referred to in the text.

We have adopted this convention throughout.

6. p15, 2nd last line of 2nd paragraph, b_f subscript missing. Also in xlabel of Fig. 6(e).

This has been corrected. We assume the reviewer was referring to Fig. 3(e).

7. p18, last sentence of 2nd paragraph, word missing.

This has been corrected.

8. p20, 2nd last sentence, word(s) missing.

This sentence has been replaced.

Reviewer #2: The Authors have answered most of my points sufficiently. I can recommend the Ms for publication. The minor points that should be corrected before the publication are as follows:

- On pg. 15, ln. 7-8, the Authors say "Though the results presented focus only on deterministic
dynamics, we note that the introduction of noise into the system leaves the qualitative picture unchanged.". Such statement without quantitative information regarding noise magnitude doesn't give much information. The Authors should specify up to which level of noise their statement holds. The noise level added to the system can be quantified using e.g. variance or standard deviation in the same units as the external input I.

In accordance with this suggestion, we introduce the following statement into the results section:

"Though we focus here on deterministic dynamics, the effect of noise on the parameter I was tested (results not shown). Noise with standard deviation 25\% of I left the qualitative picture unchanged in that intermittent transitions with similar characteristics to the deterministic case were observed. When the standard deviation was increased to 50\% of I, transitions became less distinguishable in terms of the difference in amplitude between non-seizure and seizure periods."

- The units of I should be specified in the text body and in the Figures or Figure's legends.

This has been incorporated

- On pg. 10, ln. 5 from the bottom: "The SWD solution consists of rhythmic on/off firing of neurons in the mass at around 3/s (Fig. 4 (e)) as is commonly observed in animal models of SWD." The 3/s SWD are characteristic of human absence seizures, in typical animal models (WAG Rij, GAERS)the frequency of SWD is around 9 Hz.

We have removed the reference to 3/s here.

***2. Reviewer Suggestions**

We would like to suggest the following reviewers:

Michael Breakspear
E-mail: mbreak@unsw.edu.au

Fabrice Wendling
E-mail: fabrice.wendling@univ-rennes1.fr

Gustavo Deco
E-mail: gustavo.deco@upf.edu

Karl Friston
E-mail: k.friston@fil.ion.ucl.ac.uk

Andreas Spiegler
E-mail: spiegler@cbs.mpg.de

Research Highlights

- Background and spike-wave oscillations are described in a cortical dynamic model.
- Transitions from background to spike-wave are described at three spatial scales.
- Spatially extended background oscillations are out-of-phase, spike wave are in-phase.
- A bistability exists between these two states.
- Spatial heterogeneity yields intermittent transitions into and out of seizure.

Intermittent spike-wave dynamics in a heterogeneous, spatially extended neural mass model

Marc Goodfellow[a,1], Kaspar Schindler[b], Gerold Baier[a]

[a] *Doctoral Training Centre Integrative Systems Biology from Molecules to Life, Manchester Interdisciplinary Biocentre, The University of Manchester, Manchester M1 7DN, UK.*

[b] *qEEG group, Department of Neurology, Inselspital, Bern University Hospital, University of Bern, Switzerland.*

Abstract

Generalised epileptic seizures are frequently accompanied by sudden reversible transitions from low amplitude irregular background activity to high amplitude, regular spike-wave discharges (SWD) in the EEG. The underlying mechanisms responsible for SWD generation and for the apparently spontaneous transitions to SWD and back again are still not fully understood. Specifically, the role of spatial cortico-cortical interactions in ictogenesis is not well studied.

We present a macroscopic, neural mass model of a cortical column which includes two distinct time scales of inhibition. This model can produce both an oscillatory background and a pathological SWD rhythm. We demonstrate that coupling two of these cortical columns can lead to a bistability between out-of-phase, low amplitude background dynamics and in-phase, high amplitude SWD activity. Stimuli can cause state-dependent transitions from background into SWD. In an extended local area of cortex, spatial heterogeneities in a model parameter can lead to spontaneous reversible transitions from a desynchronised background to synchronous SWD due to intermittency. The deterministic model is therefore capable of producing absence seizure-like events without any time dependent adjustment of model parameters.

[1]Corresponding Author: Marc Goodfellow, Manchester Interdisciplinary Biocentre, The University of Manchester, Manchester M1 7DN, UK. Phone: +44 (0) 161 3065124, fax: +44 (0)161 3064556, email: marc.goodfellow@postgrad.manchester.ac.uk

The emergence of such mechanisms due to spatial coupling demonstrates the importance of spatial interactions in modelling ictal dynamics, and in the study of ictogenesis.

Keywords: Mathematical modelling, Neural-mass models, Absence epilepsy, EEG, Spike-wave discharge, Ictogenesis

---

1. Introduction

Spike and wave discharges (SWD) are electrographic features commonly recorded on the EEG during a variety of generalised epileptic events, including absence seizures, myoclonic seizures and seizures of the Lennox-Gestaut syndrome (see e.g. Hrachovy and Frost 2006). The importance of this generic waveform in brain dysfunction has led to intense investigation of the underlying neuronal mechanisms in a number of different animal models of SWD seizures (Gloor et al., 1977; Marescaux and Vergnes, 1995; Steriade and Contreras, 1998; Coenen and Van Luijtelaar, 2003). A ubiquitous finding from these models is that of increased synchronous firing of cortical neurons during the "spike", followed by relative quiescence during the "wave".

(Electro-) physiological investigations of animal models have been supplemented by mathematical modelling studies of the processes underlying SWD generation, particularly with respect to the putative thalamo-cortical network interactions thought to underlie the 3/s SWD of typical absence seizures, or the 9/s correlate in rat models (Destexhe, 1998; Suffczynski et al., 2004; Traub et al., 2005; Breakspear et al., 2006; Sargsyan et al., 2007; Marten et al., 2009a). Such approaches allow the investigation of SWD generating mechanisms at the systems level, i.e. at the level of complex interactions between the diverse range of processes known to underlie brain (dys-) function. In this way one can test hypotheses about the relative importance of these different processes for the generation of pathological macroscopic brain activity. For example, epileptic rhythms are underpinned by hyperpolarising and depolarising mechanisms (McCormick and Contreras, 2001) including, but not restricted to, synaptic interactions between excitatory and inhibitory neurons. These interactions have been incorporated into mathematical models of both focal onset seizures (Wendling et al., 2002; Labyt et al., 2006) and generalised seizures with SWD (Destexhe, 1998; Breakspear et al., 2006; Suffczynski et al., 2004; Marten et al., 2009b). In particular, the inclusion of different time scales of synaptic inhibition (Thomson and Deuchars, 1997) in these models has been important, although controversy remains over the relative importance of synaptic inhibitory processes in determining the rhythmic firing observed to underlie scalp SWD (Charpier et al., 1999; Timofeev et al., 2004; Bazhenov et al., 2008).

Models of thalamocortical network interactions underlying the generation of SWD represent an examination of a restricted set of the important mechanisms that may underlie ictogenesis and the emergence of epileptic SWD.

In particular, the majority of connectivity within the cortex is of cortico-cortical origin (Douglas and Martin, 2007) and therefore one can assume that this connectivity plays an important role at least with respect to propagation of epileptic rhythms in the cortex. In addition, the mechanisms of SWD events in certain animal models are known to be predominantly of a cortical origin (Steriade and Contreras, 1998). Thus a more complete understanding of ictogenic processes will come from mathematical models incorporating these connections. However, the complex nature of neuronal connectivity in the cortex makes this a difficult task. In particular, a detailed characterisation of neuronal interactions over an extended region of cortex will result in an extremely large model in terms of number of variables and parameters (Markram, 2006). Drawbacks of such an approach include vast computational demands, difficulties in parameterisation and an inability to characterise system dynamics over changes in parameters. These drawbacks can be overcome by modelling at the macroscopic level, with variables and parameters accounting for averages over large local networks of neurons, thus providing a parsimonious way with which to study spatially extended interactions (Wilson and Cowan, 1973; Lopes Da Silva et al., 1974; Amari, 1977; Jansen and Rit, 1995).

Previous macroscopic models of SWD generation or ictogenesis in generalised seizures (Suffczynski et al., 2004; Breakspear et al., 2006) have not accounted explicitly for extended cortico-cortical connectivity. The model of Breakspear et al. (2006) was derived from spatially extended interactions in the cortex (a cortical field approach), though the transition to SWD was examined in a globally homogeneous mode. In the model of Suffczynski et al. (2004), a single thalamocortical network was studied, with no spatial extension in the cortex besides the local population of cortical neurons. However, macroscopic models incorporating cortico-cortical connectivities at a variety of scales do exist (Wilson and Cowan, 1973; Amari, 1977; Jansen and Rit, 1995; David and Friston, 2003; Sotero et al., 2007; Babajani-Feremi and Soltanian-Zadeh, 2010; Ursino et al., 2010). In particular, the model of Jansen and Rit (1995) incorporates a means to connect different cortical compartments and has been exploited as such in the study of mechanisms underlying rhythm generation in focal epilepsies (Labyt et al., 2006).

In this study we introduce a model of SWD in a cortical mass, which is based upon the model of Jansen and Rit (1995). In order to generate rhythmic on/off firing we introduce a fast and a slow time scale of inhibition, which initially are tuned to replicate firing patterns observed during 3/s

absence seizures. We demonstrate that in a single compartment, the model is capable of displaying both fast "background", low amplitude oscillations and high amplitude SWD with approximately 3/s neuronal firing. We then examine modes of transition from background to SWD at 3 spatial scales, expanding sequentially from a single model to 2 coupled compartments and finally a larger model. We demonstrate that spatial connections are important for ictogenesis in this model and in examining larger, heterogeneous systems, demonstrate that spontaneous transition in and out of intermittent seizure events can arise. Thus, this spatially extended, heterogeneous, macroscopic model provides a new dynamical route to spontaneous epileptic seizure activity.

2. Methods

2.1. Model

We use the model of cortical neural mass activity of Jansen (Jansen et al., 1993; Jansen and Rit, 1995). For a detailed description, a schematic of the structure of this model and the physiological interpretation of output variables we refer the reader to the main text and Fig. 1 of Jansen and Rit (1995) and, for example, the detailed description of Wendling et al. (2002). In brief, the model in its original form captures, in three coupled impulse response equations (six differential equations), a feedback network between principal neurons, inhibitory interneurons and excitatory interneurons within a local cortical mass, i.e. at the macroscopic scale.

The model has been researched extensively in studies of evoked EEG responses (Zavaglia et al., 2006; David et al., 2005), functional connectivity (Wendling et al., 2001; David et al., 2004) and whole brain dynamics (Sotero et al., 2007; Babajani-Feremi and Soltanian-Zadeh, 2010). It has also been extensively applied to the investigation of focal epilepsies (Wendling et al., 2002; Labyt et al., 2006; Cosandier-Rimélé et al., 2008). These latter studies have seen the original form of the Jansen model extended to include many other physiologically relevant aspects of neuronal activity. In particular, versions of this model designed to account for ictal dynamics in partial seizures have included different time scales of inhibitory activity in the hippocampus (Wendling et al., 2002) and cortex (Labyt et al., 2006), with the latter model incorporating a slow inhibitory time scale mediated by $GABA_b$ inhibition. In this study we introduce a simple extension to the original Jansen model by including a second, slow inhibitory post-synaptic potential (IPSP) on the

pyramidal neurons. The model structure is therefore close to that used by Wendling et al. (2002), though we omit the interactions between inhibitory processes that were inferred specifically for hippocampal activity.

In the current study we also incorporate N interacting local populations of neurons. The model connectivity is given according to the original work of Jansen (Jansen and Rit, 1995), whereby populations communicate via excitatory input from other principal neurons. However, explicit time delays are neglected as we restrict the model here to interacting *local* populations, residing below a single recording site. Investigations of inhibitory connectivity, longer range interactions and considerations of multiple recording scalp electrodes are left to further studies.

Each population, defined by superscript i, is modelled by a system of 8 differential equations representing the interaction of excitatory and inhibitory cortical processes (Jansen et al., 1993; Jansen and Rit, 1995), with model equations given by:

$$
\begin{aligned}
\dot{y_0^i}(t) &= y_4^i(t) \\
\dot{y_4^i}(t) &= AaS[y_1^i(t) - 0.5y_2^i(t) - 0.5y_3^i(t)] - 2ay_4^i(t) - a^2y_0^i(t) \\
\dot{y_1^i}(t) &= y_5^i(t) \\
\dot{y_5^i}(t) &= Aa\{I + P^i + C_2S[C_1y_0^i(t)]\} - 2ay_5^i(t) - a^2y_1^i(t) \\
\dot{y_2^i}(t) &= y_6^i(t) \\
\dot{y_6^i}(t) &= B_fb_f\{C_4S[C_3y_0^i(t)]\} - 2b_fy_6^i(t) - b_f^2y_2^i(t) \\
\dot{y_3^i}(t) &= y_7^i(t) \\
\dot{y_7^i}(t) &= B_sb_s\{C_4S[C_3y_0^i(t)]\} - 2b_sy_7^i(t) - b_s^2y_3^i(t)
\end{aligned}
$$

Inter-compartment connectivity is defined by a homogeneous connectivity constant, R, representing coupling between different local populations. The input to each population, P^i $(i = 1, .., N)$ is therefore given by the weighted contribution of all other populations, as shown below:

$$
P^i = \sum_{j=1, j\neq i}^{N} \frac{R}{N-1} S[y_1^j - 0.5y_2^j - 0.5y_3^j]
$$

We therefore use 4 blocks of impulse response equations (see e.g. Jansen and Rit (1995)) to represent changes in the membrane potential of interneurons (1 block, output variable y_0) and pyramidal neurons (3 blocks, output variables y_1,y_2 and y_3). Within the model a net post-synaptic potential (PSP) is transformed via the sigmoidal activation function $S[v]$ (Marreiros et al., 2008) into pyramidal neuronal activity or firing rate:

$$S[v] = 2e_0/(1 + \exp(r(v_0 - v)));$$

2.2. Model parameters

The excitatory post-synaptic potential (EPSP) has the same time scale and amplitude parameters as the original model (Jansen and Rit, 1995). For the inhibitory processes, we set a fast and a slow time scale and tune the amplitude using the original parameter ratios (Jansen and Rit, 1995) as utilised in David and Friston (2003) and Spiegler et al. (2010). We note the use of different time scale and gain parameters for the inhibitory processes in this study compared to Wendling et al. (2002). Time courses of inhibitory synaptic processes have been shown to be highly variable and to lie in a range between lengths of the order of 20 ms (Thomson and Deuchars, 1997) and 500 ms (Otis et al., 1993). The time course of the slow IPSP used here is of the order of 300 ms (see Fig. 1) and is thus within this physiologically plausible range. Furthermore, both of our IPSP time scale parameters reside within a physiologically plausible range suggested for time scale parameters of the Jansen model in a recent study (Spiegler et al., 2010).

We maintain the original internal connectivity ratios used to calculate $C1$ through $C4$. The total connectivity, given by C and the input parameter I are varied throughout the paper, though within ranges of previous publications (e.g. Jansen and Rit 1995; Wendling et al. 2002; Labyt et al. 2006). Parameters of the sigmoid function are the same as those used in previous incarnations of this model (Jansen and Rit, 1995). Fig. 1 shows the time profile of the PSPs used in the model and Table 1 lists parameter values used in this study.

FIGURE 1 here

Parameter	Description	Value
A	Average excitatory gain	3.25mV
B	Average fast inhibitory gain	44mV
B_s	Average slow inhibitory gain	8.8mV
a	Average excitatory time constant	$100s^{-1}$
b_f	Average fast inhibitory time constant	100s^{-1}
b_s	Average slow inhibitory time constant	20s^{-1}
C, C_1, C_2	Connectivity constants	C is varied, $C_1 = C, C_2 = 0.8C$
C_3, C_4		$C_3 = C_4 = 0.25C$
I	External input to pyramidal neurons	I is varied
R	Matrix of connectivity constants	R is varied though is homogeneous.
v_0	Parameters of the sigmoid function	$v_0 = 6\text{mV}$
e_0, r		$e_0 = 2.5s^{-1}, r = 0.56\text{mV}^{-1}$

Table 1: Parameter values used for all output shown in this study. The fast and slow inhibitory gain parameters were derived by fixing the respective time scales and then deriving the gain from the ratio B/b, as suggested by David and Friston (2003).

2.3. Analysis

Solutions of the model were explored by plotting bifurcation diagrams of time series maxima and minima over changes in parameters I, C, b_f and R. I represents input into the system and has been explored in previous bifurcation analyses (Grimbert and Faugeras, 2006; Spiegler et al., 2010), C and R represent connectivity within and between cortical masses (Jansen and Rit, 1995), respectively, and are thus of interest in relation to ictogenesis. The time scale of fast inhibition, here represented by b_f, has been shown to be variable in experimental studies (Thomson and Deuchars, 1997). For each of these bifurcation diagrams, the presence of different solutions was determined by evaluating the model over increasing and decreasing values of one of these parameters, with all other parameters fixed. Relevant solutions identified by this procedure were allocated distinct marker types, as shown in Fig. 3. In systems of multiple compartments, maxima and minima plots were given for one compartment only, though we note in each case qualitatively similar diagrams were obtained for the remaining compartments. In this case, we also calculated the distribution of pair-wise phase differences between compartments over a 2 second window using the Hilbert transform. The mean phase difference was plotted over the range of bifurcation parameter, with solution type extracted by inspection. Thus, in all bifurcation plots,

regions of bistability were uncovered by forward and backward parameter scans, with markers allocated on plots by visual inspection of the time series of each solution.

In the spatially extended, heterogeneous models, the amplitude of the time series provided a good distinction between seizure (turbulent) and non-seizure (laminar) phases (see Figs. 9 (b) and 10 (a)). It was observed that seizure periods predominantly carried amplitudes greater than 10, whereas non-seizure periods were of a much lower amplitude. Since each of these simulations was at least 1000 seconds in length, it was decided that phase lengths would be determined at a resolution of 1 second. The lengths of laminar and turbulent phases were therefore characterised by whether the maximum amplitude was greater than 10 in non-overlapping windows of 1 second length.

3. Results

The results section is divided into three parts, representing an investigation of model dynamics at three different spatial scales. Section 1 deals with a model of a single compartment, section 2 considers two coupled compartments, and finally, section 3 explores the dynamics of a model of a small cortical region composed of twenty five connected compartments. In Fig. 2 we provide a peri-ictal recording of frontal scalp electrode EEG during absence seizure in order to demonstrate several important clinical features of these events and also to facilitate comparisons with features of the model transitions described. In particular we note the apparently spontaneous transition from low amplitude oscillatory background dynamics into high amplitude SWD activity and back again.

FIGURE 2 here

3.1. One compartment

The dynamics of the one compartment model were explored numerically by evaluating model output over a range of a selection of system parameters (see section "2.3. Analysis"). The effect of changes in I, C and b_f are shown in the bifurcation diagrams of Fig. 3. Fig. 3 (a), (b) and (c) show model dynamics over changes in I for C=190, 220 and 240 respectively. It can be seen that different system behaviours emerge for different combinations

of I and C. In particular, the system is capable of displaying fixed point (thin lines, single maxima, "Fp", Fig. 3), sinusoidal limit cycle oscillations (henceforth referred to as "background" oscillations, marked as "Bckg", open circles Fig. 3), SWD (marked as "SWD", stars in Fig. 3), poly-SWD (marked as "pSWD", open squares in Fig. 3) and "other oscillations" (marked as "O1", "O2" and "O3", grey lines, Fig. 3). Exemplary time series for each of these solutions are given in Fig. 3 (f), which also serves as a legend for this and subsequent bifurcation diagrams (Fig. 6 and Fig. 8). Maxima and minima of the SWD solution are identical in the forward and backward scan. Note that there are two minima and two maxima per spike wave complex.

For small values of C, solutions are either fixed point or background oscillations (Fig. 3 (a)). There is a region of bistability between these two solutions for small I at C=190 (Fig. 3 (a), "BS1"). The SWD solution emerges for larger C (Fig. 3 (b), "SWD") and widens over I as C increases (Fig. 3 (b), (c)). The amplitude of the background oscillations is consistently smaller than that of the SWD. There is also the emergence of poly-SWD behaviour for large I and C (Fig. 3 (b), "BS3" and Fig. 3 (c), "pSWD").

With I fixed at 135 s^{-1}, dynamics over changing C are shown in Fig. 3 (d). As C increases the system moves from fixed point to background oscillations and then into SWD for large C. With C fixed at 190, dynamics over changing b_f are shown in Fig. 3 (e). It can be seen that low values of b_f result in a large amplitude slow oscillation (Fig. 3 (e), "O3"), whereas intermediate values produce SWD dynamics. As b_f nears the default parameter value of 100 s^{-1} the system passes through a region of bistability between SWD and background oscillations (Fig. 3 (e), "BS8"). Though several other small regions of bistability were encountered (Fig. 3 (b) "BS2", Fig. 3 (c), "BS4" and "BS5", Fig. 3 (c), "BS6" and "BS7"), the default parameter values used throughout this study placed the one compartment system into a monostable regime, with respect to the parameters investigated. These default parameter values are indicated by vertical lines in Fig. 3.

Fig. 4 shows details of two of the oscillatory solutions in the model, namely the SWD and the background oscillation, which are the focus of this study. The SWD solution consists of rhythmic on/off firing of neurons in the mass (Fig. 4 (e)) as is commonly observed in animal models of SWD. The SWD waveform carries contributions from all three underlying PSPs, with increased EPSP and firing during the positive (downwards) deflection and quiescence of firing during the "wave" (Fig. 4 (c), (e)). The background solution also has rhythmic firing at a faster frequency (approximately 15Hz,

Fig. 4 (f)), though firing is not "on/off" as it reaches neither the maximum nor minimum firing capability. The Fourier spectrum of the SWD (Fig. 4 (g)) shows a dominant peak at 2.5 Hz and a number of harmonics due to the nonlinear waveform. The Fourier spectrum of the background oscillations (Fig. 4 (h)) has its main peak at 15 Hz.

There exist several modes of transition into SWD dynamics within this model. In Fig. 5, we demonstrate two possible such transitions, namely i) a ramping of parameter C for fixed I and ii) a perturbation of the input parameter I. Fig. 5 (a) shows a model time series under the ramp in parameter C, which is displayed in Fig. 5 (b). In the "pre-seizure" state, the system oscillates at the background frequency. As C starts to increase the amplitude of the oscillation increases and at a threshold level of C the spike-wave oscillation is activated. When the control parameter crosses the critical point the dynamics return to the original background oscillation. The bistability (Fig. 3 (d) "BS7") seen for changing C means that the threshold level on the way up and the critical point on the way down are not equivalent.

To demonstrate transition ii), with the system in the background oscillation state (e.g. C=190, I=135 s^{-1}), a finite pulse of short duration (see section "3.2. Two compartments") was applied. Depending on the phase at which this pulse was delivered, the system could respond with a transient single spike-wave oscillation before returning to the background oscillation. An example of this behaviour is shown in Fig. 5 (c), with stimulus time indicated by an arrow.

FIGURE 3 here

FIGURE 4 here

FIGURE 5 here

3.2. Two compartments

To investigate the effect of spatial interactions in this model, the dynamics of a system of two coupled compartments was explored (Fig. 6). Here, C was fixed at 190, which in the one compartment model resulted in background oscillations or a fixed point (see Fig. 3 (a)). In this regime, the effect of the input parameter, I, was explored for different coupling strengths, with

bifurcation diagrams of time series minima over changing I shown for two of the investigated values, R= 25 and R=50 in Fig. 6 (a) and (b), respectively.

In the two compartment model we observed each of the dynamics observed in the single compartment model. In addition to the qualitative differences in waveforms observed with changing parameter values, which can be represented by standard bifurcation plots of time series extrema (of one compartment only, Fig. 6 (a) and (b)), qualitative differences also emerged in terms of synchrony between the two compartments. This was manifest by differences in both amplitude and phase. In order to represent these effects, plots of phase difference between the two compartments are shown in Fig. 6 (c) and (d) (see section "2.3. Analysis").

At a coupling value of R=25 (Fig. 6 (a)), a region of bistability between background and SWD oscillations emerges (Fig. 6, (a) "BS9"). We note that since the uncoupled individual compartments are set into the background oscillation regime (see Fig. 3, vertical lines), this new behaviour is entirely the result of spatial coupling. In addition, the SWD solution is always homogeneous in the two compartments (Fig. 6 (c), zero phase difference for SWD solution in region "BS9"), whereas the background solution in this region is always heterogeneous (Fig. 6 (c), open circles). In this case (as well as in the qualitatively similar solution Fig. 6 (d)) there exists a second solution with waveforms exchanged between compartments due to the symmetry of the model. We note that the power spectrum of the mean field of the SWD solution and the background solution are comparable to the one compartment case (Fig. 4). For higher values of I, less sinusoidal "other" oscillations emerge, initially out of phase and with a periodic amplitude modulation, then settling to higher amplitude, in-phase solutions for larger I.

At R=50, SWD and pSWD solutions are identical in both compartments (Fig. 6 (b) and (d)). A region of bistability exists for intermediate I between identical pSWD and out of phase "other" oscillations (Fig. 6 (b), "BS10"). The insets of Fig. 6 (c) and (d) indicate the nature of two of the out of phase solutions.

The bistable region between low amplitude, heterogeneous background oscillations and high amplitude, homogeneous SWD found for R=25 represents a good model to study perturbation-induced transitions. The nature of such a transition in the model was explored by means of a stimulus to the input (I) of the model in its background state (Fig. 7), with C=190 and initially I=135 s^{-1}.

The nature of model evolution post stimulus depended upon the strength,

timing and duration of stimulus, and could either result in a return to background (sometimes accompanied by a switch in amplitudes (high vs. low) between the two compartments, results not shown) or transient or permanent SWD. In order to investigate these possibilities, the stimulus duration and amplitude were fixed (duration = 0.1s, amplitude = 300), and the effects of stimulus timing were explored. Results for two different stimulus times are given in Fig. 7. The times relative to phase of underlying activity are shown by vertical bars in Fig. 7 (a).

In the case that the model eventually returned to the background state, this invariably evolved via a transient of SWD activity. The length of this transient event, and also the degree to which the two compartments were synchronised during the transient period was found to be variable and dependent upon the state of the system at time of stimulus. An example of such a transient, resulting in a two second "seizure" is shown in Fig. 7 (b). The underlying model PSPs for the onset and offset of SWD activity in this transient are shown in Fig. 7 (c) and (d). It can be seen that the stimulus provides an increase in magnitude of all internal PSPs and results in an increased contribution of the slow IPSP, relative to the fast IPSP, thus starting the cycle of slow IPSP activation (dashed line) and subsequent system rebound. The offset, or transition from SWD to background activity stems from a rebound of activity before the end of the slow IPSP (Fig. 7 (d)). In this case, immediate post-SWD compartments are in anti-phase and settle back to the heterogeneous background state. The stimulus could also provide immediate transition into permanent SWD (Fig. 7 (e)).

FIGURE 6 here

FIGURE 7 here

3.3. Twenty-five compartments

The relevance of these results to larger cortical regions was explored by investigating a model consisting of twenty-five compartments with homogeneous (all-to-all) coupling (see section "2.1. Model"). Here, we fixed C=190 and I=135 s^{-1}, and explored the dynamics of the system under changing R. Maxima and minima are plotted for one of the twenty-five compartments in the bifurcation diagram of Fig. 8 (a). For low R, the system displayed out of phase background oscillations, which developed a quasiperiodic (amplitude

modulated) dynamics with increasing R (Fig. 8 (a), "Bckg" and "pBckg"). We stress that although this region with periodic amplitude modulation may look like a noise artefact, it is actually representative of certain periods during the time course in which the amplitude in all compartments undergoes a smooth increase and decrease. For higher R, the model produced a region of bistability (Fig. 8 (a), "BS11"), again between in phase SWD and out of phase background oscillations (phase-locked or quasi-periodic). For values $R > 40$ the synchronised spike-wave is the only stable solution. The phase relationships for each of these solutions are represented in Fig. 8 (b) as the mean of the distribution of pair-wise phase differences (see section "2.3. Analysis"). We note that in this and in the two compartment case, a small random error term was added to the initial conditions of each compartment prior to simulation in order that the compartments were not simply starting from identical initial conditions.

With reference to the results of Fig. 7 in the two compartment case, we note that in the twenty-five compartment model in the region of bistability "BS11" in Fig. 8 a pulse perturbation to the background oscillation most often elicited only a single SWD. However, more complex perturbations, for example a train of two consecutive pulses, could lead to longer transient SWD trains or permanent SWD.

It is expected that spatially extended regions of cortex will not be homogeneous either in terms of connectivity or intrinsic dynamics. In order to investigate the effect of heterogeneity in our local cortical model, a random value drawn from a normal distribution was added to the time scale parameter of the fast IPSP. This attempts to reflect the array of fast inhibitory time scales observed in neocortex (Thomson and Deuchars, 1997). The dynamics of the resulting system of non-identical compartments is explored in Figs. 9 and 10. We found that the system could either display stable background oscillations, stable SWD oscillations or intermittent SWD trains of varying lengths and frequency of occurrence. Intermittency is an important type of dynamics in deterministic nonlinear models (see e.g. Berge et al. (1987) for an accessible introduction based on low-dimensional discrete dynamical systems). Intermittency is defined as the spontaneous switching between a (quasi-) regular (or laminar) phase of dynamics (in our case the background oscillations) and irregular outbursts of a second type of dynamics (in our case SWD). Different types of intermittency are classified according to the local instability of a periodic orbit using Floquet multipliers (Berge et al., 1987). This means that the SWD spike trains occur at irregular intervals

and with irregular duration due to the intrinsic model dynamics and do not require parameter changes or additional noise terms in the model. Though we focus here on deterministic dynamics, the effect of noise on the parameter I was tested (results not shown). Noise with standard deviation 25% of I left the qualitative picture unchanged in that intermittent transitions with similar characteristics to the deterministic case were observed. When the standard deviation was increased to 50% of I, transitions became less distinguishable in terms of the difference in amplitude between non-seizure and seizure periods.

In an initial investigation of long simulations (200 seconds) of this heterogeneous system we noted that the mean value of b_f was smaller on occasions leading to the intermittent solution, and that in particular, values $b_f < 90$ s^{-1} in a number of compartments conferred either permanent SWD or intermittent dynamics. To clarify this point we made 50 long simulations, each of 10,000 seconds duration and each with a random normal distribution of b_f parameters, centred at b_f=100 s^{-1} and with standard deviation $b_f/10$=10. We categorised each of these simulations as either permanent SWD (Fig. 9 (a), black regions), permanent BG (Fig. 9 (a), white regions) or intermittent seizures (Fig. 9 (a), grey regions) (see section "2.3. Analysis"). Fig. 9 (a) shows the distribution of number of compartments with $b_f < 90$ s^{-1} for each of the aforementioned categories. It is clear that there is a systematic increase in propensity for SWD activity when a greater number of compartments have $b_f < 90$ s^{-1}. Note that in a single compartment, values less than 90 s^{-1} for b_f lead to SWD rather than background activity (see Fig. 3 (e)).

To study the nature of the intermittent seizure activity, we present in Fig. 9 (b) 5000 seconds of one of the intermittent solutions. This solution corresponds to a single point in parameter space. The horizontal lines provide a guide to the amplitude cut off used to distinguish SWD from background. In this example, a long simulation producing in excess of 1000 seizures provided a mean seizure duration of 8 seconds and a mean inter-seizure duration of 74 seconds. Following the analysis of intermittency in EEG from rat models of absence seizures (Hramov et al., 2006; Velazquez et al., 1999), we analysed the type of intermittency by examining the distribution of lengths of the laminar phase (Fig. 9 (c)) and by plotting a second return map of model amplitude for the laminar phase (Fig. 9 (d)). Fig. 9 (c) shows the distribution of laminar lengths on a log-log scale, overlayed on which is the gradient -1.5 expected for the case of parametrically driven one-dimensional maps with on-off intermittency (Heagy et al., 1994). Fig. 9 (c) therefore demonstrates

that this specific instance of our model is not consistent with power law scaling. Power law scaling is only expected close to the onset of intermittent behaviour (Chate and Manneville, 1987). In addition, the study of Hramov et al. (2006) demonstrated deviations from the power law under certain experimental conditions. A more complete understanding of the intermittency in our model and the relevance of this to experimental findings can therefore only be found with a full characterisation of the distributions with respect to its parameter space. The second return map of the laminar phases shows a noisy distribution of maxima (Fig. 9 (d)). This is in disagreement with any of the types of intermittency that follow local bifurcations (e.g. type III intermittency) and in agreement with intermittencies associated with a global bifurcation.

One of the seizures from an intermittent solution is explored further in Fig. 10. Fig. 10 (a), shows the mean field model EEG during the seizure period, calculated as the average output of all 25 compartments. It can be seen that this mode of transition from background oscillation to synchronous SWD is comparable to the real seizure event shown in Fig. 2 in terms of the change in amplitude and also the spontaneous onset and offset of SWD.

Overlaid on Fig. 10 (a) are a succession of grids indicating the involvement of SWD in each of the twenty-five compartments during six five-second windows. The grids are colour coded to indicate the presence of SWD at some point during the window in each compartment, with grey indicating that a SWD oscillation was present. This was achieved by comparing the average time series maxima in this epoch against the mean from a known "seizure-free" period. Each grid represents the five second window at which it is located between the tick marks on the horizontal axis. It can be seen that in the pre-ictal and post-ictal periods, a small number of compartments are involved in intermittent SWD and that this behaviour is generalised over the whole local system during seizure. We note that the grey shading does not indicate that the compartment produced persistent SWD in this period, rather it indicates the presence of at least one SWD. Fig. 10 (b),(c) and (d) show close ups of model time series at seizure onset, middle of seizure and seizure offset, respectively. Before seizure onset, most of the compartments oscillate without SWD dynamics, though the waveform of oscillations is heterogeneous due to the variance in time scale parameter. Occasional SWD also appear in some time series. During seizure, however, most compartments are clustered into SWD activity. The heterogeneity in time scales can still be observed in the slight differences between SWD waveforms, though the activity

remains predominantly phase locked. At the end of the seizure, this synchronous activity breaks apart as more compartments revert to background oscillations.

Fig. 10 (e) shows a close up of the mean field model activity during the seizure, in which it can be seen that the underlying heterogeneity causes a fragmentation of the "clean" SWD waveform. For comparison, a segment of EEG recording during a typical absence seizure is shown in Fig. 10 (g). Though the mean field model captures well the fragmentation of the wave observed in the real recording, the spike part of the SWD in the model is truncated. However, if an alternative conversion of model output to EEG is used (Goodfellow et. al. submitted), in which the internal model variables carry adjusted weights, the dynamics of the real EEG can be matched more closely. This is demonstrated by the model output of Fig. 10 (f) in which the amplitude of spike relative to wave and the waveform in general closely resembles the recorded time series. In this case, certain deformations of the "classical" waveform, such as the introduction of small spikes into the wave, are captured by the model.

Interestingly, the power spectrum of the "pre-seizure" model mean field has a region of dominant power between 9 and 13 Hz. The power spectrum reflects the desynchronised irregular background dynamics. Due to the ergodic properties of the deterministic dynamical system, each of the compartments would have a similar power spectrum if evaluated over a very long time. However, on short time scales, the power spectrum of an individual compartment is typically more peaked than the spectrum of the mean field signal. This is in contrast to the background solution of the one compartment case which has a single peak at 15Hz (Fig. 4). In the SWD region, the power spectrum peak has increased to approximately 3.2Hz and associated harmonics. However, due to the variability in waveform in the heterogeneous system, peaks are slightly broadened.

FIGURE 8 here

FIGURE 9 here

FIGURE 10 here

4. Discussion

We have shown that a cortical neural mass model containing two explicitly modelled time scales of inhibition can produce slow SWD as well as sinusoidal background oscillations, thus providing the means for a parameter driven transition to seizure. Exploration of dynamics in coupled models revealed that spatial extensions could in addition confer spontaneous transitions from irregular cortical background to synchronised spike-wave dynamics.

The single compartment model was capable of producing low amplitude oscillatory and high amplitude SWD or poly-SWD dynamics. The SWD oscillations were accompanied in the model by rhythmic on/off firing as is ubiquitously observed in recordings from animal models of SWD (Gloor et al., 1977; Marescaux and Vergnes, 1995; Steriade and Contreras, 1998; Coenen and Van Luijtelaar, 2003). This firing pattern was mediated by the increased relative contribution of the slow IPSP, whereas in the background state, a faster frequency of oscillation was present. We note that the frequency of this background oscillation was of the same order of magnitude as the spike of the SWD, as observed, for example, in the frequency of the fast runs that lead to SWD in a feline model of SWD (Steriade et al., 1998a).

A transition between background oscillations and SWD dynamics could be observed with an increase in C for fixed input (Fig. 5). This parameter encompasses the magnitude of connectivity within a neural mass (Jansen and Rit, 1995) and increasing its value results in two effects on system dynamics. Firstly, activated excitatory and inhibitory interneurons move position in the sigmoid function towards higher voltages and therefore are more excitable in the sense that their firing rate is higher in the linear part of the sigmoid activation function, or closer to activation in the non-firing part of this curve. Secondly, the firing rate of these neurons is scaled to provide an increased input into the PSPs of the principal neurons. Indeed, increasing C with constant input led to an increase in magnitude of oscillations in internal PSPs (data not shown). In this sense, an increase in C encompasses a notion of enhanced local excitability, which has been postulated during seizure states in animal models (Steriade et al., 1998a; Polack et al., 2007). Alternatively, individual spike wave responses could be induced transiently by means of a short stimulus (Fig. 5 (c)). This was further explored in a spatially extended version of the single-compartment model.

We demonstrated that a spatial extension to this model confers the system with additional dynamics (Fig. 6), including the existence of a region of

bistability between background oscillations and SWD. In addition to differences in waveform and frequency between the two solutions in this parameter region, there was also a difference in the phase relationship between the two compartments of the model, namely that background oscillations were out of phase whereas SWD were in phase. This is equivalent to the dynamics of brain activity during absence seizures in animal model studies, in which the seizure state is accompanied by time locked firing of cortical neurons relative to more diffuse temporal relationships during background activity (Steriade and Amzica, 1994; Neckelmann et al., 1998). The large amplitude observed on scalp EEG during SWD seizures is also indicative of a significantly increased degree in time synchrony of underlying neuronal activity compared to a background state.

The existence of a region of bistability between these two states indicates a capability of the system to undergo spontaneous transitions into and out of seizures. This property could be important, for example, in explaining the spontaneous transition from background EEG into 3/s SWD activity as seen in absence seizures (Lopes da Silva et al., 2003). Indeed, a previous model of the thalamocortical network was demonstrated to be capable of noise-induced transitions in a region of bistability between a fixed point and limit cycle with relevant power spectra (Suffczynski et al., 2004). In contrast, a different thalamocortical model demonstrated a transition from background to SWD that was mediated by smooth changes in model output with the dynamic modulation of a relevant model parameter (Breakspear et al., 2006). In terms of system dynamics, the 2 compartment model presented here makes notable improvements on these previous studies by reconciling i) an oscillatory background state, ii) a relevant difference between the phase relationship of background and seizure oscillations and iii) bistability between background and SWD oscillations. We therefore present important new tools in the investigation of SWD generating mechanisms from the non-linear dynamics perspective. A noise driven oscillatory background state has been assumed in a large number of previous studies (see e.g. Jansen and Rit 1995; David and Friston 2003; Wendling et al. 2002), whereas a previous mathematical model of absence seizures assumed the background to be a noise driven steady state in order to account for the irregularity of background EEG (Breakspear et al., 2006). While our two compartment model is more regular than clinical background EEG, we address this point by suggesting that the recorded EEG signal is in fact a mean over a larger number of coupled compartments. For example, the disorganised or complex oscillations in the mean field of the

25 compartment model provides an alternative explanation for observations likening background EEG to filtered noise.

Cortical stimulation has been shown to elicit seizure activity in the feline model of SWD seizures (Steriade et al., 1998a). We investigated this mode of transition to SWD in the model by applying a short time dependent rise in the input parameter, I. It was shown that such stimuli could lead either to prolonged (permanent) SWD dynamics or a transient period of SWD which decayed to the background state (Fig. 7). The fate of the system subsequent to stimulus depended upon, amongst other factors, the state of the system at time of stimulus. System evolution post-stimulus differed in terms of length of seizure activity and degree of homogeneity in output between the two compartments, resulting in fragmentation of the SWD. Such variability is often observed on human EEG recorded during absence seizures (Sadleir et al. 2006 and Fig. 10 (g)).

In the study of (Steriade et al., 1998a), the authors hypothesised that stimulating fast bursting neurons would be particularly effective in generating spatially extended pathological oscillations, presumably via synaptic connectivity, just as in our model the two compartments interact via excitatory connectivity to synchronise in SWD. However, we note that in our model, onset of seizure activity was predominantly instant, whereas in the feline model repeated stimulus was required for a time delayed transition to seizure. These differences can probably be explained by our simplistic model of local interactions which does not incorporate the extensive and complex activity of the brain *in vivo*.

An extended area of cortex was modelled by a network of twenty-five reciprocally connected compartments. We observed that this configuration with heterogeneous fast inhibitory time scales could display intermittent seizure activity in the mean field. We stress that no time dependent noise term was applied to the model in order to mediate these transitions, which therefore provide a means of SWD onset and offset not previously reported in modelling studies of SWD to our knowledge.

The simulation depicted in Fig. 9 (b) over a longer duration possessed mean seizure and non-seizure lengths of 8 and 74 seconds, respectively, both of which values are in line with analysis of recordings from the WAG/Rij rat model of absence seizures (Akman et al., 2010; Hramov et al., 2006). Previous studies have attempted to classify the nature of intermittency in both human epilepsy and animal model EEG. Velazquez et al. (1999) described type III (low dimensional) intermittency both in fast spiking recordings from human

partial epilepsy and in SWD during temporal lobe epilepsy (Velazquez et al., 2003). EEG of rats with genetic absence epilepsy, on the other hand, have been reported to be of the on-off type (Hramov et al., 2006). This latter characterisation was made by comparison to a power law distribution with exponent -1.5. However, alternative analyses of ictal and inter-ictal phase duration have hypothesised exponential or gamma distributions (Suffczynski et al., 2004, 2006). The results of our phase length and second return map in a specific case (Fig. 9 (c), (d)) do not support a straight-forward categorisation of the behaviour of the single instance of our model shown. This is to be expected given that the power law holds strictly near the onset of intermittency (Chate and Manneville, 1987). Also the predictions of statistics regarding types of intermittency were derived using low dimensional space independent models (Heagy et al., 1994) or infinite dimensional partial differential equations (Chate and Manneville, 1987). In principle, the behaviour of our coupled model with its 200 variables may allow for different types of intermittent solutions which have not yet been characterised mathematically. A detailed characterisation of the bifurcation scenarios leading to the observed intermittency will provide further insight into the different types of distributions to be expected in experimental models.

Previous mathematical models displaying intermittent behaviour have been of an abstract nature (Ohayon et al., 2004). In contrast to the idea that intermittency is only found in abstract constructs (Kalitzin et al., 2010), we find that this type of dynamics can emerge when explicit spatial interactions and heterogeneities are considered in a physiologically motivated model. Thus our current model provides the means to investigate further the nature of such transitions to epileptic activity, for example in relation to stimulus feedback control (Kalitzin et al., 2010).

In addition to intermittency in model behaviour, the mean field displayed fragmentation of the SWD waveform as commonly observed in SWD of human absence seizures (Sadleir et al., 2006). We therefore propose that such fragmented SWD, or the appearance of additional "spikes" could be mediated by spatial variation in underlying pathological rhythmic activity. Interestingly, the frequency of the background model mean field consisted of peaks in the alpha range of the power spectrum as is often observed in clinical EEG. This is in contrast to the one compartment case, which possessed a single peak at 15Hz. We postulate that this more relevant frequency of background activity is due both to the heterogeneity in time scale parameters and the effect of averaging local heterogeneous compartment behaviour to form the

mean field EEG.

The background state in this heterogeneous model included intermittent or permanent pathological oscillations in a subset of model compartments. Thus, the mode of seizure onset at the macroscopic level related to the spreading of SWD rhythms from a small number of compartments to the whole system. This is in line with recent findings from animal model studies that suggest a cortical focus for the initiation of generalised seizures (Meeren et al., 2002; Polack et al., 2007). Polack et al. (2007) reported that epileptic foci were capable of producing pathological oscillations that did not become generalised seizures, which relates directly to our finding of clusters of SWD activity outside of the seizure period. However, we note that in the findings of Polack et al. (2007) such "background" pathological oscillations were not equivalent to those during the seizure periods.

Regional changes are found both structurally (Woermann et al., 1999) and functionally (Holmes et al., 2010) in human generalised epilepsy. In addition, intra-cranial recordings from human epileptic and control subjects suggest that in focal epilepsy, pathological activity or "microseizures" do exist at small spatial scales (Stead et al., 2010). This finding implies that epileptic rhythms could be an intrinsic part of healthy cortical circuits, and that icto- and epilepto-genesis are related to the ability of these pathological rhythms to spread in the cortex. Spatially extended models like the one presented here will provide the means to investigate this spread and therefore will be important in future studies of ictogenesis in both generalised and focal seizures.

Numerical integration of spatially extended dynamic models requires a compartmentalisation of the system at a chosen spatial scale. The original model of Jansen and Rit (Jansen and Rit, 1995) was formulated at the level of a cortical column (Mountcastle, 1997) incorporating local inhibitory and excitatory feedback mechanisms. It has become clear that this assumption of a well defined columnar modularity is an over simplification of the complex horizontal and laminar connectivity within different regions of the cortex (da Costa and Martin, 2010; Douglas and Martin, 2007). At the other extreme, spatially continuous approaches cannot so easily account for the observed spatially restricted activity of local neuronal subsystems. However, spatial extensions in the Jansen approach (David and Friston, 2003; Sotero et al., 2007; Babajani-Feremi and Soltanian-Zadeh, 2010; Ursino et al., 2010) allow one to model connectivity at a hierarchy of scales. Thus, if the notion of space in these models is made more abstract, so that we consider modelled

compartments to represent "canonical microcircuits" (da Costa and Martin, 2010), in the spirit of the extended model of David and Friston (2003), the effect of connectivity between heterogeneous local networks incorporating known feedback networks can be investigated. Such an approach is particularly relevant in the study of epilepsy where spatially isolated rhythm generation is an important observed phenomenon (Stead et al., 2010).

Our model incorporates excitatory and inhibitory feedback with two inhibitory time scales. The parameters of the excitatory PSP were preserved from the original model (Jansen and Rit, 1995). A wide variety of synaptic inhibitory mechanisms have been recorded in animal cortex preparations (for example Thomson and Deuchars 1997; Otis et al. 1993), some of which have been incorporated in previous models of focal epileptic dynamics (Wendling et al., 2002; Labyt et al., 2006). Since there is no consensus regarding the exact origin of the hyperpolarising wave during SWD, we fixed an arbitrary slow IPSP which, combined with the fast IPSP resulted in SWD in the region of 3/s. We therefore suggest that this longer IPSP could represent an average of fast and slow IPSPs from a variety of different inhibitory interneurons. However, there is much evidence that this rhythmic hyperpolarisation is not mediated by IPSPs, but could instead be attributable to a change in neuronal input resistance, perhaps mediated by potassium ion concentrations (Bazhenov et al., 2008). Though the model presented here is based on synaptic interactions, the principle of delayed, non-linear activation of a slow inhibitory process could provide an abstract model for non-synaptic mediated inhibition (Llinás, 1988). Furthermore, since little is known about the cellular correlates of SWD in humans, one cannot rule out the presence of a long synaptic inhibitory process. We suggest that in order to uncover further the effects of interactions between different time scales of inhibitory and excitatory processes, future neural mass modelling work should explicitly account for a wide range of inhibitory time scales (Labyt et al., 2006), representative of synaptic and non-synaptic processes. We also note that the principal aim of the current study was to investigate the importance of spatial coupling between neural masses capable of rhythmic on/off firing, rather than to uncover the exact physiological mechanisms mediating this behaviour.

Our spatial extension considered only excitatory coupling between pyramidal neurons, and therefore does not account for spatially extended synapses onto inhibitory or excitatory interneurons. In previous models, these connections, as well as interactions between different inhibitory populations, have

been shown to affect dynamics within the Jansen framework (e.g. Ursino et al. 2010). The values of the connectivity parameter, R, used in this study are difficult to relate exactly to physical coupling, though they embody a notion of number of synaptic connections between pyramidal neurons (Jansen and Rit, 1995). We note that these values of R are within bounds used in the study of Ursino et al. (2010).

In this study we have considered only cortical mechanisms for the onset of pathological activity. However, subcortical structures are thought to play an ictogenic role in some epilepsies. Despite reports of cortical initiation of absence seizures (Meeren et al., 2002; Polack et al., 2007, 2009), for example, it is accepted that thalamic mechanisms are necessary for the development of SWD in certain animal models (Meeren et al., 2009). In fact, absence seizures are understood to be a disorder of thalamocortical network interactions (Blumenfeld, 2005). A limitation of the current model in explaining absence seizure ictogenesis in particular is the exclusion of a thalamic component interacting with the cortex, as is presented in the models of Suffczynski et al. (2004) and Breakspear et al. (2006). A natural extension to the current model is therefore the addition of a thalamic component, as provided in a recent study of whole brain dynamics within the neural mass model framework (Sotero et al., 2007). An extension of the model into a larger cortical domain would also provide further insight into the role of hierarchies of cortical connectivity in ictogenesis. Such large scale neural mass models have previously been reported (Sotero et al., 2007; Babajani-Feremi and Soltanian-Zadeh, 2010), as has the importance of forward models in comparing simulations to empirical EEG data (Cosandier-Rimélé et al., 2008). A large-scale extension of the model presented here, combined with a forward model to EEG, may provide insight into the nature of cortical dynamics underlying heterogeneous SWD recordings of human absence seizures (Weir, 1965; Cohn and Leader, 1967; Lemieux and Blume, 1986; Rodin and Ancheta, 1987; McKeown et al., 1999).

To summarise, we have demonstrated that important dynamic features of epileptic EEG may emerge from a mathematical model with explicit spatial interactions. In particular, the spatial extension can lead to intermittent seizure periods when parameter distributions are heterogeneous. In recreating relevant aspects of background and SWD dynamics reported in humans and animal models, we thus provide a framework with which to better understand ictogenesis in terms of spatio-temporal cortical mechanisms.

5. Acknowledgements

The authors thank Hiltrud Muhle, Ulrich Stephani, University Hospital Schleswig-Holstein, for additional absence seizure data. We also thank Peter Taylor for useful suggestions regarding bifurcation plots. MG acknowledges financial support from EPSRC and BBSRC through the Doctoral Training Centre Integrative Systems Biology from Molecules to Life. GB acknowledges financial support from EPSRC and BBSRC and thanks Ulrich Stephani, Hiltrud Muhle and Michael Siniatchkin for discussions.

References

Akman, O., Demiralp, T., Ates, N., Onat, F. Y., 2010. Electroencephalographic differences between WAG/Rij and GAERS rat models of absence epilepsy. Epilepsy Research 89 (2-3), 185–193.

Amari, S., 1977. Dynamics of pattern formation in lateral-inhibition type neural fields. Biol Cybern 27 (2), 77–87.

Babajani-Feremi, A., Soltanian-Zadeh, H., 2010. Multi-area neural mass modeling of EEG and MEG signals. NeuroImage, 1–19.

Bazhenov, M., Timofeev, I., Fröhlich, F., Sejnowski, T. J., 2008. Cellular and network mechanisms of electrographic seizures. Drug Discov Today Dis Models 5 (1), 45–57.

Berge, P., Pomeau, Y., Vidal, C., 1987. Order within chaos: Towards a deterministic approach to turbulence. Wiley-Interscience.

Blumenfeld, H., 2005. Cellular and network mechanisms of spike-wave seizures. Epilepsia 46, 21–33.

Breakspear, M., Roberts, J. A., Terry, J. R., Rodrigues, S., Mahant, N., Robinson, P. A., 2006. A Unifying explanation of primary generalized seizures through nonlinear brain modeling and bifurcation analysis. Cereb Cortex 16, 1296–1313.

Charpier, S., Leresche, N., Deniau, J., Mahon, S., Hughes, S., Crunelli, V., 1999. On the putative contribution of $GABA_B$ receptors to the electrical events occuring during spontaneous spike and wave discharges. Neuropharmacology 38 (11), 1699–1706.

Chate, H., Manneville, P., 1987. Transition to turbulence via spatio-temporal intermittency. Physical Review Letters 58 (2), 112–115.

Coenen, A. M. L., Van Luijtelaar, E. L. J. M., 2003. Genetic animal models for absence epilepsy: a review of the WAG/Rij strain of rats. Behav Genet 33 (6), 635–55.

Cohn, R., Leader, H. S., 1967. Synchronization characteristics of paroxysmal EEG activity. Electroencephalogr Clin Neurophysiol 22 (5), 421–8.

Cosandier-Rimélé, D., Merlet, I., Badier, J. M., Chauvel, P., Wendling, F., 2008. The neuronal sources of EEG: modeling of simultaneous scalp and intracerebral recordings in epilepsy. NeuroImage 42 (1), 135–46.

da Costa, N. M., Martin, K. A. C., 2010. Whose cortical column would that be? Front Neuroanat 4, 16.

David, O., Cosmelli, D., Friston, K. J., 2004. Evaluation of different measures of functional connectivity using a neural mass model. NeuroImage 21, 659 – 673.

David, O., Friston, K. J., 2003. A neural mass model for MEG/EEG: coupling and neuronal dynamics. Neuroimage 20 (3), 1743–55.

David, O., Harrison, L., Friston, K. J., 2005. Modelling event-related responses in the brain. NeuroImage 25 (3), 756–770.

Destexhe, A., 1998. Spike-and-wave oscillations based on the properties of $GABA_B$ receptors. J Neurosci 18 (21), 9099.

Douglas, R. J., Martin, K. A. C., 2007. Recurrent neuronal circuits in the neocortex. Curr Biol 17 (13), R496–500.

Gloor, P., Quesney, L. F., Zumstein, H., 1977. Pathophysiology of generalized penicillin epilepsy in the cat: the role of cortical and subcortical structures. ii. topical application of penicillin to the cerebral cortex and to subcortical structures. Electroencephalogr Clin Neurophysiol 43 (1), 79–94.

Grimbert, F., Faugeras, O., 2006. Bifurcation analysis of jansen's neural mass model. Neural Comput 18 (12), 3052–68.

Heagy, J., Platt, N., Hammel, S., 1994. Characterization of on-off intermittency. Physical Review E 49 (2), 1140–1150.

Holmes, M. D., Quiring, J., Tucker, D. M., 2010. Evidence that juvenile myoclonic epilepsy is a disorder of frontotemporal corticothalamic networks. Neuroimage 49 (1), 80–93.

Hrachovy, R. A., Frost, Jr, J. D., 2006. The EEG in selected generalized seizures. J Clin Neurophysiol 23 (4), 312–32.

Hramov, A., Koronovskii, A. A., Midzyanovskaya, I. S., Sitnikova, E., van Rijn, C. M., 2006. On-off intermittency in time series of spontaneous paroxysmal activity in rats with genetic absence epilepsy. Chaos 16 (4).

Jansen, B., Zouridakis, G., Brandt, M., 1993. A neurophysiologically-based mathematical model of flash visual evoked potentials. Biol Cybern 68 (3), 275–283.

Jansen, B. H., Rit, V. G., 1995. Electroencephalogram and visual evoked potential generation in a mathematical model of coupled cortical columns. Biol Cybern 73, 357–366.

Kalitzin, S. N., Velis, D. N., da Silva, F. H. L., 2010. Stimulation-based anticipation and control of state transitions in the epileptic brain. Epilepsy & Behavior 17 (3), 310–323.

Labyt, E., Uva, L., de Curtis, M., Wendling, F., 2006. Realistic modeling of entorhinal cortex field potentials and interpretation of epileptic activity in the guinea pig isolated brain preparation. J Neurophysiol 96, 363–377.

Lemieux, J., Blume, W., 1986. Topographical evolution of spike-wave complexes. Brain Res. 373 (1-2), 275–287.

Llinás, R. R., 1988. The intrinsic electrophysiological properties of mammalian neurons: insights into central nervous system function. Science 242 (4886), 1654–64.

Lopes da Silva, F., Blanes, W., Kalitzin, S. N., Parra, J., Suffczynski, P., Velis, D. N., 2003. Epilepsies as dynamical diseases of brain systems: basic models of the transition between normal and epileptic activity. Epilepsia 44 Suppl 12, 72–83.

Lopes Da Silva, F., Hoeks, A., Smits, H., Zetterberg, L., 1974. Model of brain rhythmic activity the ralpha-rhythm of the thalamus. Kybernetik 15, 27–37.

Marescaux, C., Vergnes, M., 1995. Genetic absence epilepsy in rats from strasbourg (GAERS). Ital J Neurol Sci 16 (1-2), 113–8.

Markram, H., 2006. The blue brain project. Nat Rev Neurosci 7 (2), 153–60.

Marreiros, A. C., Daunizeau, J., Kiebel, S. J., Friston, K. J., 2008. Population dynamics: variance and the sigmoid activation function. Neuroimage 42 (1), 147–57.

Marten, F., Rodrigues, S., Benjamin, O., Richardson, M. P., Terry, J., 2009a. Onset of polyspike complexes in a mean-field model of human electroencephalography and its application to absence epilepsy. Philos. Transact. A Math. Phys. Eng. Sci. 367 (1891), 1145–1161.

Marten, F., Rodrigues, S., Suffczynski, P., Richardson, M. P., Terry, J. R., 2009b. Derivation and analysis of an ordinary differential equation mean-field model for studying clinically recorded epilepsy dynamics. Phys Rev E Stat Nonlin Soft Matter Phys 79 (2 Pt 1), 021911.

McCormick, D. A., Contreras, D., 2001. On the cellular and network bases of epileptic seizures. Annu Rev Physiol 63, 815–46.

McKeown, M., Humphries, C., Iragui, V., Sejnowski, T., 1999. Spatially fixed patterns account for the spike and wave features in absence seizures. Brain Topogr 12 (2), 107–116.

Meeren, H. K. M., Pijn, J. P. M., Van Luijtelaar, E. L. J. M., Coenen, A. M. L., Lopes da Silva, F. H., 2002. Cortical focus drives widespread corticothalamic networks during spontaneous absence seizures in rats. J Neurosci 22 (4), 1480–95.

Meeren, H. K. M., Veening, J. G., Möderscheim, T. A. E., Coenen, A. M. L., van Luijtelaar, G., 2009. Thalamic lesions in a genetic rat model of absence epilepsy: dissociation between spike-wave discharges and sleep spindles. Exp Neurol 217 (1), 25–37.

Mountcastle, V. B., 1997. The columnar organization of the neocortex. Brain 120 (Pt 4), 701–22.

Neckelmann, D., Amzica, F., Steriade, M., 1998. Spike-wave complexes and fast components of cortically generated seizures. iii. synchronizing mechanisms. J Neurophysiol 80 (3), 1480–94.

Ohayon, E., Kalitzin, S., Suffczynski, P., Jin, F., Tsang, P., Borrett, D., Burnham, W., Kwan, H., 2004. Charting epilepsy by searching for intelligence in network space with the help of evolving autonomous agents. Journal of Physiology-Paris 98 (4-6), 507–529.

Otis, T. S., De Koninck, Y., Mody, I., 1993. Characterization of synaptically elicited gabab responses using patch-clamp recordings in rat hippocampal slices. J Physiol 463, 391–407.

Polack, P.-O., Guillemain, I., Hu, E., Deransart, C., Depaulis, A., Charpier, S., 2007. Deep layer somatosensory cortical neurons initiate spike-and-wave discharges in a genetic model of absence seizures. J Neurosci 27 (24), 6590–9.

Polack, P.-O., Mahon, S., Chavez, M., Charpier, S., 2009. Inactivation of the somatosensory cortex prevents paroxysmal oscillations in cortical and related thalamic neurons in a genetic model of absence epilepsy. Cereb Cortex 19 (9), 2078–91.

Rodin, E., Ancheta, O., 1987. Cerebral electrical fields during petit-mal abscences. Electroencephalogr. Clin. Neurophysiol. 66 (6), 457–466.

Sadleir, L. G., Farrell, K., Smith, S., Connolly, M. B., Scheffer, I. E., 2006. Electroclinical features of absence seizures in childhood absence epilepsy. Neurology 67 (3), 413–8.

Sargsyan, A., Sitnikova, E., Melkonyan, A., Mkrtchian, H., van Luijtelaar, G., 2007. Simulation of sleep spindles and spike and wave discharges using a novel method for the calculation of field potentials in rats. J Neurosci Methods 164 (1), 161–76.

Sotero, R. C., Trujillo-Barreto, N. J., Iturria-Medina, Y., Carbonell, F., Jimenez, J. C., 2007. Realistically coupled neural mass models can generate EEG rhythms. Neural Comput 19 (2), 478–512.

Spiegler, A., Kiebel, S. J., Atay, F. M., Knösche, T. R., 2010. Bifurcation analysis of neural mass models: Impact of extrinsic inputs and dendritic time constants. Neuroimage 52 (3), 1041–58.

Stead, M., Bower, M., Brinkmann, B. H., Lee, K., Marsh, W. R., Meyer, F. B., Litt, B., Van Gompel, J., Worrell, G. A., 2010. Microseizures and the spatiotemporal scales of human partial epilepsy. Brain.

Steriade, M., Amzica, F., 1994. Dynamic coupling among neocortical neurons during evoked and spontaneous spike-wave seizure activity. Journal of Neurophysiology 72 (5), 2051–2069.

Steriade, M., Amzica, F., Neckelmann, D., Timofeev, I., 1998a. Spike-wave complexes and fast components of cortically generated seizures. ii. extra- and intracellular patterns. J Neurophysiol 80 (3), 1456–79.

Steriade, M., Contreras, D., 1998. Spike-wave complexes and fast components of cortically generated seizures. i. role of neocortex and thalamus. J Neurophysiol 80 (3), 1439–55.

Suffczynski, P., Kalitzin, S., Lopes Da Silva, F., 2004. Dynamics of non-convulsive epileptic phenomena modeled by a bistable neuronal network. Neuroscience 126 (2), 467–484.

Suffczynski, P., Lopes da Silva, F. H., Parra, J., Velis, D. N., Bouwman, B. M., van Rijn, C. M., van Hese, P., Boon, P., Khosravani, H., Derchansky, M., Carlen, P., Kalitzin, S., 2006. Dynamics of epileptic phenomena determined from statistics of ictal transitions. IEEE Trans Biomed Eng 53 (3), 524–32.

Thomson, A. M., Deuchars, J., 1997. Synaptic interactions in neocortical local circuits: dual intracellular recordings in vitro. Cereb Cortex 7 (6), 510–22.

Timofeev, I., Grenier, F., Steriade, M., 2004. Contribution of intrinsic neuronal factors in the generation of cortically driven electrographic seizures. J Neurophysiol 92 (2), 1133–43.

Traub, R. D., Contreras, D., Cunningham, M. O., Murray, H., LeBeau, F. E. N., Roopun, A., Bibbig, A., Wilent, W. B., Higley, M. J., Whittington, M. A., 2005. Single-column thalamocortical network model exhibiting gamma oscillations, sleep spindles, and epileptogenic bursts. J Neurophysiol 93 (4), 2194–232.

Ursino, M., Cona, F., Zavaglia, M., 2010. The generation of rhythms within a cortical region: analysis of a neural mass model. Neuroimage 52 (3), 1080–94.

Velazquez, J., Cortez, M., Snead, O., Wennberg, R., 2003. Dynamical regimes underlying epileptiform events: role of instabilities and bifurcations in brain activity. Physica D-Nonlinear Phenomena 186 (3-4), 205–220.

Velazquez, J. L., Khosravani, H., Lozano, A., Bardakjian, B. L., Carlen, P. L., Wennberg, R., 1999. Type iii intermittency in human partial epilepsy. Eur J Neurosci 11 (7), 2571–6.

Weir, B., 1965. The morphology of the spike-wave complex. Electroencephalogr Clin Neurophysiol 19 (3), 284–290.

Wendling, F., Bartolomei, F., Bellanger, J., Chauvel, P., 2002. Epileptic fast activity can be explained by a model of impaired GABAergic dendritic inhibition. Eur J Neurosci 15 (9), 1499–1508.

Wendling, F., Bartolomei, F., Bellanger, J. J., Chauvel, P., 2001. Interpretation of interdependencies in epileptic signals using a macroscopic physiological model of the EEG. Clin Neurophysiol 112 (7), 1201–18.

Wilson, H. R., Cowan, J. D., 1973. A mathematical theory of the functional dynamics of cortical and thalamic nervous tissue. Kybernetik 13 (2), 55–80.

Woermann, F., Free, S., Koepp, M., Sisodiya, S., Duncan, J., 1999. Abnormal cerebral structure in juvenile myoclonic epilepsy demonstrated with voxel-based analysis of MRI. Brain 122, 2101–2107.

Zavaglia, M., Astolfi, L., Babiloni, F., Ursino, M., 2006. A neural mass model for the simulation of cortical activity estimated from high resolution EEG during cognitive or motor tasks. J Neurosci Methods 157 (2), 317–29.

Figure captions

Figure 1:
Time course of the three PSPs used in the model of section 2.1 with R=0: EPSP (solid line), fast IPSP (dot-dashed line) and slow IPSP (dashed line).

Figure 2:
20 second extract of a clinical absence seizure recorded from a frontal electrode. Negativity is plotted upwards by convention.

Figure 3:
Bifurcation diagrams showing model dynamics of a single compartment (maxima and minima) over changes in I, C and b_f. (a), (b) and (c) show dynamics for changing I at C=190, 220 and 240, respectively. (d) shows dynamics for changing C with I fixed at 135 s^{-1}. (e) shows dynamics for changing b_f with I=135 s^{-1} and C=190. (f) shows 6 solutions along with the marker style used to represent them. For clarity, background (Bckg), SWD (SWD), poly SWD (pSWD) and other (O1, O2 and O3) solutions are also indicated by text labels on each figure, as are regions of bistability (BS1 to BS7). The location of parameter values used in later parts of the study are indicated by vertical lines.

Figure 4:
Properties of two of the oscillatory model solutions in the one compartment model. The left column (a, c, e, g) represents the SWD solution (C=220, I=135 s^{-1}) whereas the right column (b, d, f, h) represents the background oscillation (C=190, I=135 s^{-1}). (a) and (b) show model time series (1 second and 0.5 seconds, respectively), (c) and (d) show internal PSPs, (coded as in Fig. 1), (e) and (f) show firing rate of principal neurons (minimum is 0 and maximum is 5) and (g) and (h) show normalised power spectra.

Figure 5:
Transitions from background (C=190, I=135 s^{-1}) to SWD in the one compartment model. (a) shows model time series output as C changes according

to the profile in (b). (c) shows the emergence of a SWD oscillation after perturbation from the background state with a finite pulse (strength I=300 s^{-1}, duration 0.15 seconds, onset at 5 seconds).

Figure 6:
Bifurcation diagrams showing model dynamics in a system of two coupled compartments over increasing I for different values of R. C is fixed at 190. (a) represents dynamics at R=25, whereas (b) represents R=50. Maxima and minima are plotted using the same markers as in Fig. 3, and are plotted for one compartment only. Bistable regions of interest are marked BS8 and BS9. (c) and (d) represent phase differences between the two compartments over the same ranges of I used in (a) and (b) (see section "2.3. Analysis"). Example time series for the out of phase solutions are shown in the insets of (c) and (d) at parameter locations indicated by arrows.

Figure 7:
Effect of transient stimulus (strength I=300, duration 0.1 seconds) to the background state (C=190, I=135 s^{-1}, R=25) of the two compartment model. (a) shows a close up of the two compartments with stimulus times indicated by vertical lines. (b) shows model evolution for stimulus 1, both compartments are plotted, one solid and one dashed. (c) and (d) show close ups of underlying PSPs at onset of stimulus and offset of the transient SWD. PSPs are coded as in Fig. 1, and are plotted for compartment one only for clarity. (e) shows model evolution for stimulus 2. Stimulus times are indicated by arrows.

Figure 8:
Bifurcation diagram over coupling strength for the homogeneous 25 compartment model (C=190, I=135 s^{-1}). In (a), maxima and minima are plotted for one compartment only, for clarity. Symbols are as in previous figures. "pBckg" indicates the start of a solution in which the background oscillation undergoes periodic amplitude modulation and leads to multiple circular markers per value of R. A bistable region is marked BS10. (b) shows the average pair-wise phase difference between all 25 compartments over changing R. Different symbols indicate different solutions as in Fig. 3 (open circles are

background, stars are SWD). Exemplary background solutions are given as insets in (b) at parameter locations indicated by arrows.

Figure 9:
Statistics relating to model intermittency. 50 long runs of 10,000 seconds length were simulated, each with a randomly drawn spatial distribution of b_f. Other parameters were homogeneous (C=190, I=135 s^{-1}, R=45). Each of the 50 simulations were classified as either "no seizure" ((a), white regions), "intermittent seizure" ((a), grey regions) or "always seizure" ((a), black seizures). (a) displays the relationship between the number of compartments allocated a value of b_f less than 90 s^{-1} and the number of solutions in each category. (b) shows a 5,000 second extract from one of the intermittent solutions. Horizontal lines are drawn at plus and minus 5 around the mean as a guide to the amplitude cut-off for seizure identification (see section "2.3. Analysis"). (c) shows the distribution of laminar phase lengths for an extended time series (containing more than 1200 seizures) of the solution in (b), along with a line showing a slope of -1.5 for comparison. (d) shows a second return map for maxima of the laminar phases of the solution plotted in (b).

Figure 10:
Intermittent SWD in a heterogeneous model of 25 compartments (C=190, I=135 s^{-1}, R=50). (a) shows an example of an intermittent model SWD event, spontaneously arising from background. The insets of (a) are grid layouts of the 25 compartments for 6 five-second windows through the time series, at the time locations indicated by position of the grid on the horizontal axis. Grey indicates the presence of SWD during the window, whereas white indicates no SWD, based on a comparison of amplitude with the average of a known background state. For example, the first grid of 25 squares represents the state of all 25 compartments between t=90 and t=95 seconds. (b), (c) and (d) show two seconds of underlying time series for seizure onset, seizure, and seizure offset respectively. Not all 25 time series are plotted here for clarity. (e) shows a close up of the model output during seizure. (f) shows the same model dynamics as (e) under an alternative conversion to EEG output (see text). (g) shows a clinical EEG recording from a frontal electrode during absence seizure.

5. Figure

Click here to download high resolution image

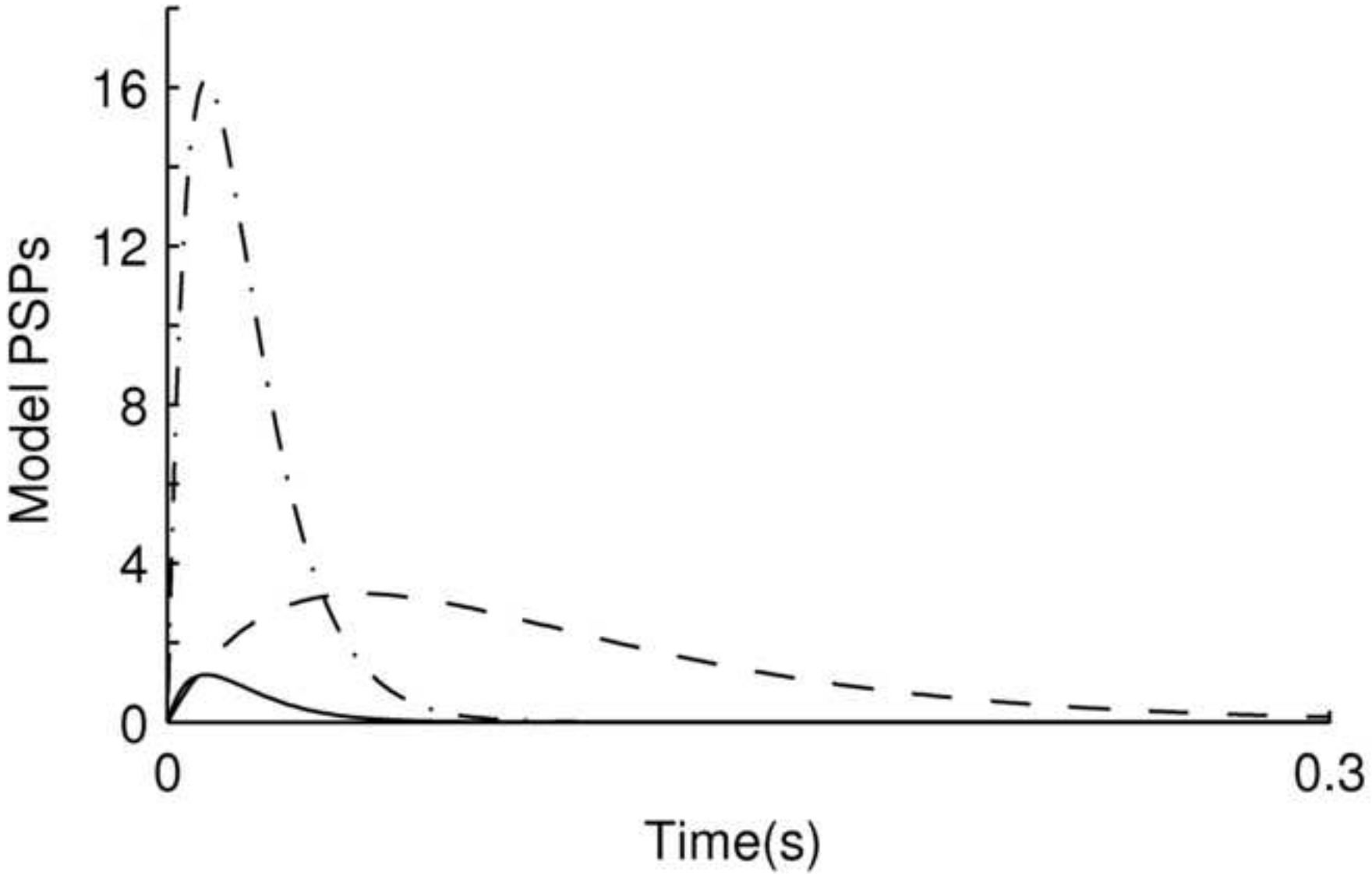

5. Figure

Click here to download high resolution image

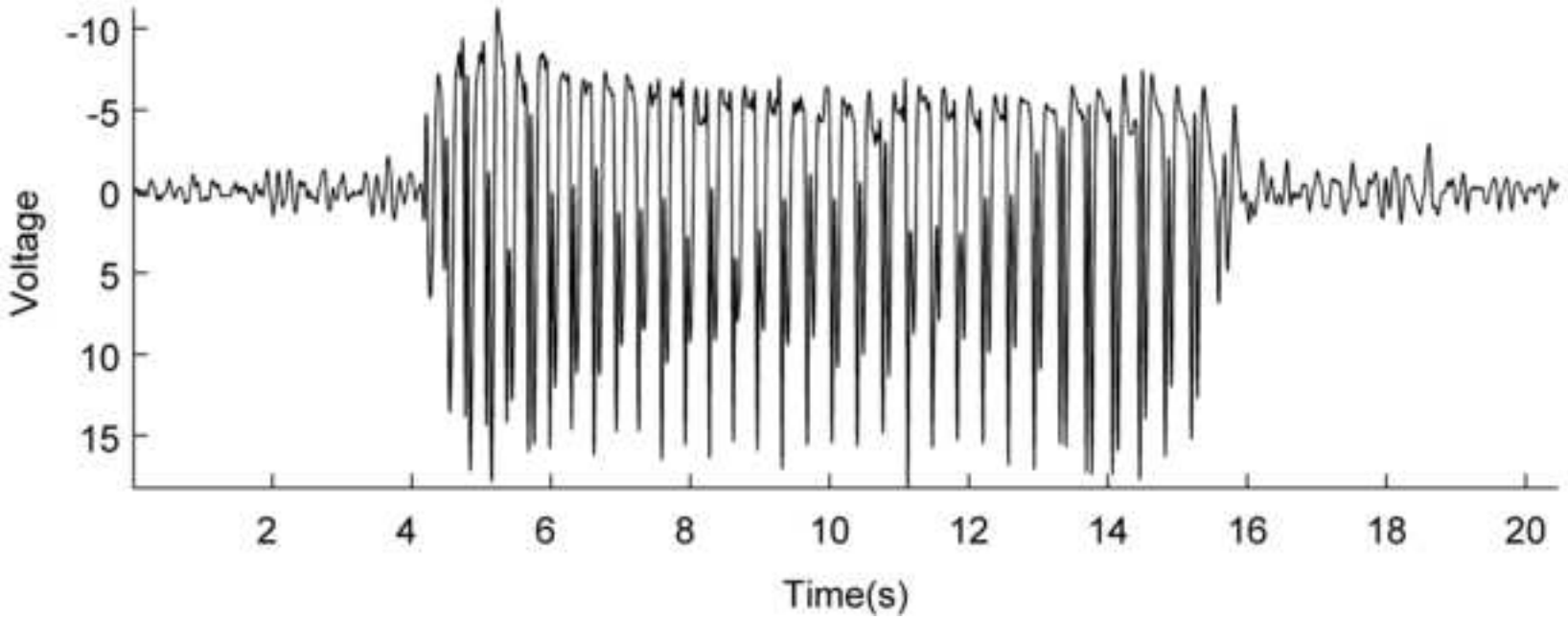

5. Figure

Click here to download high resolution image

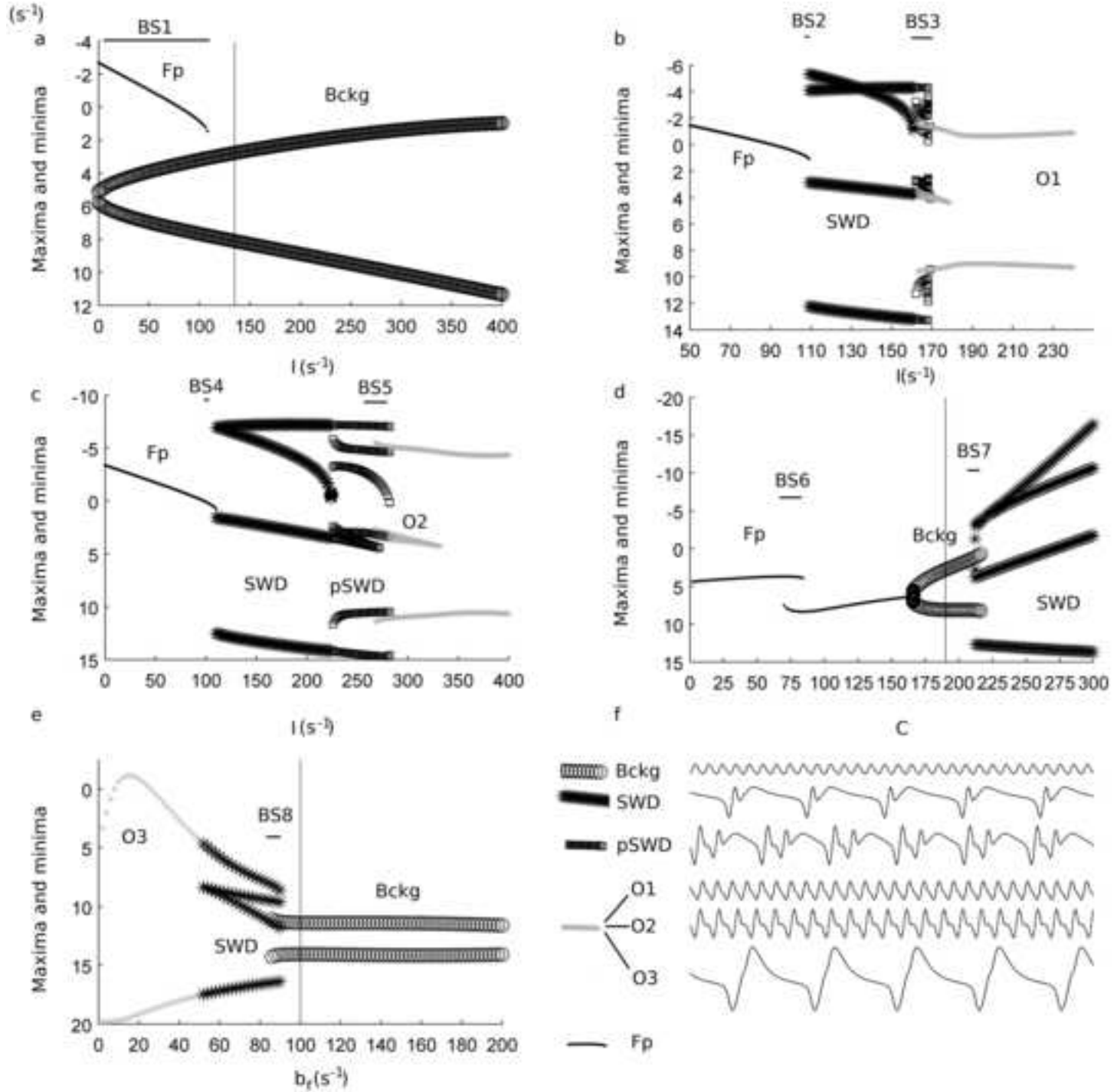

5. Figure

Click here to download high resolution image

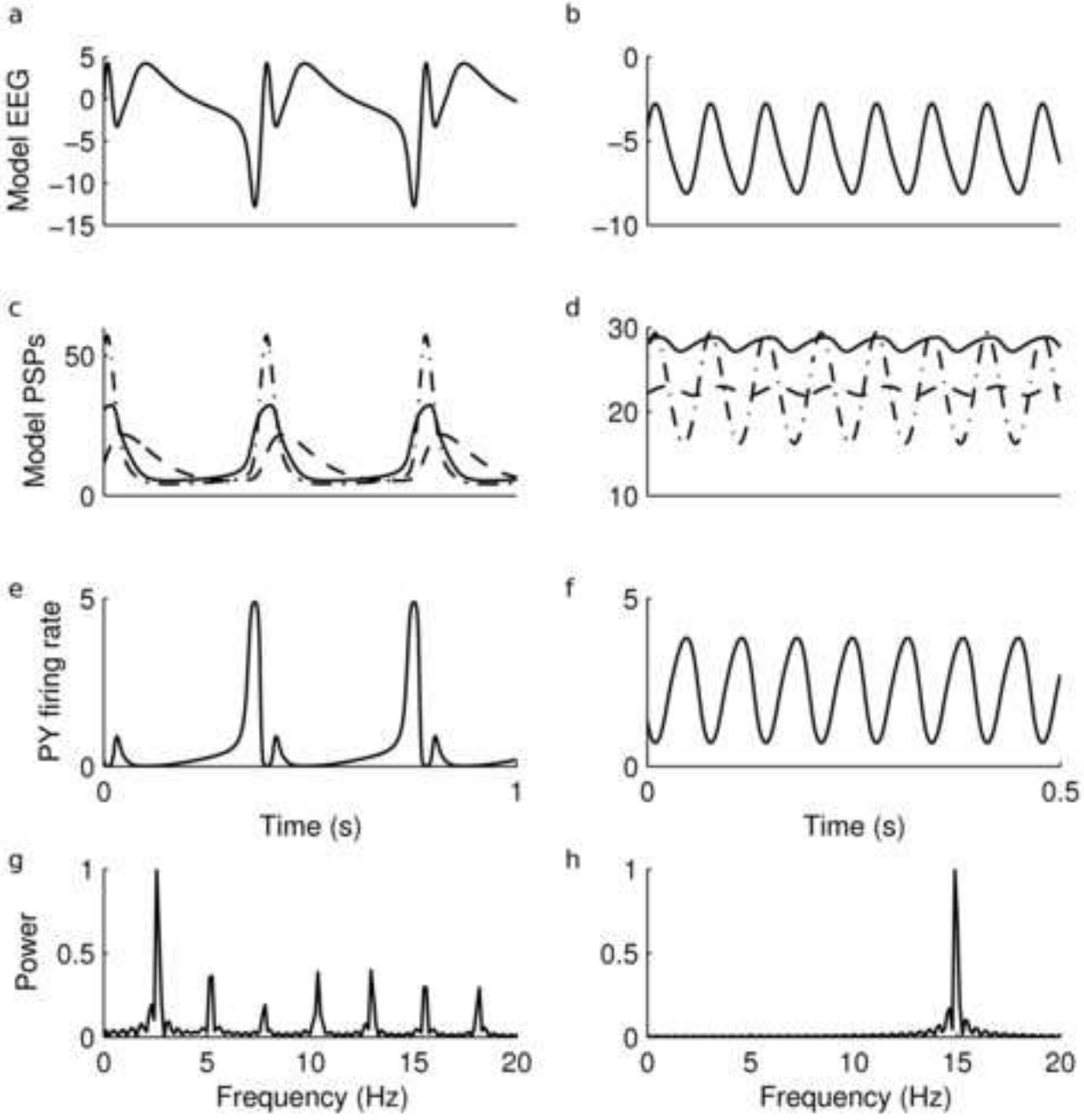

5. Figure

Click here to download high resolution image

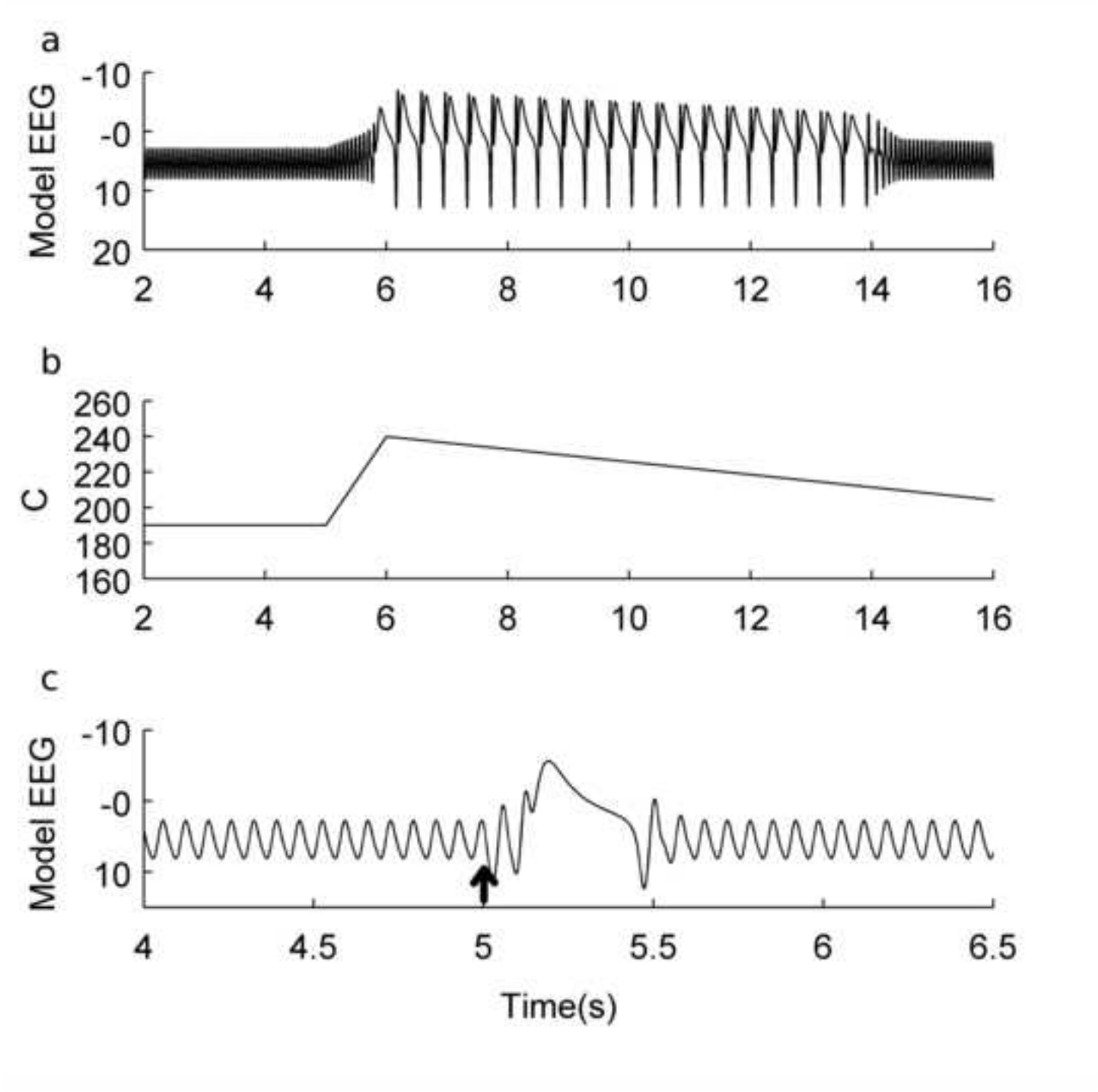

5. Figure

Click here to download high resolution image

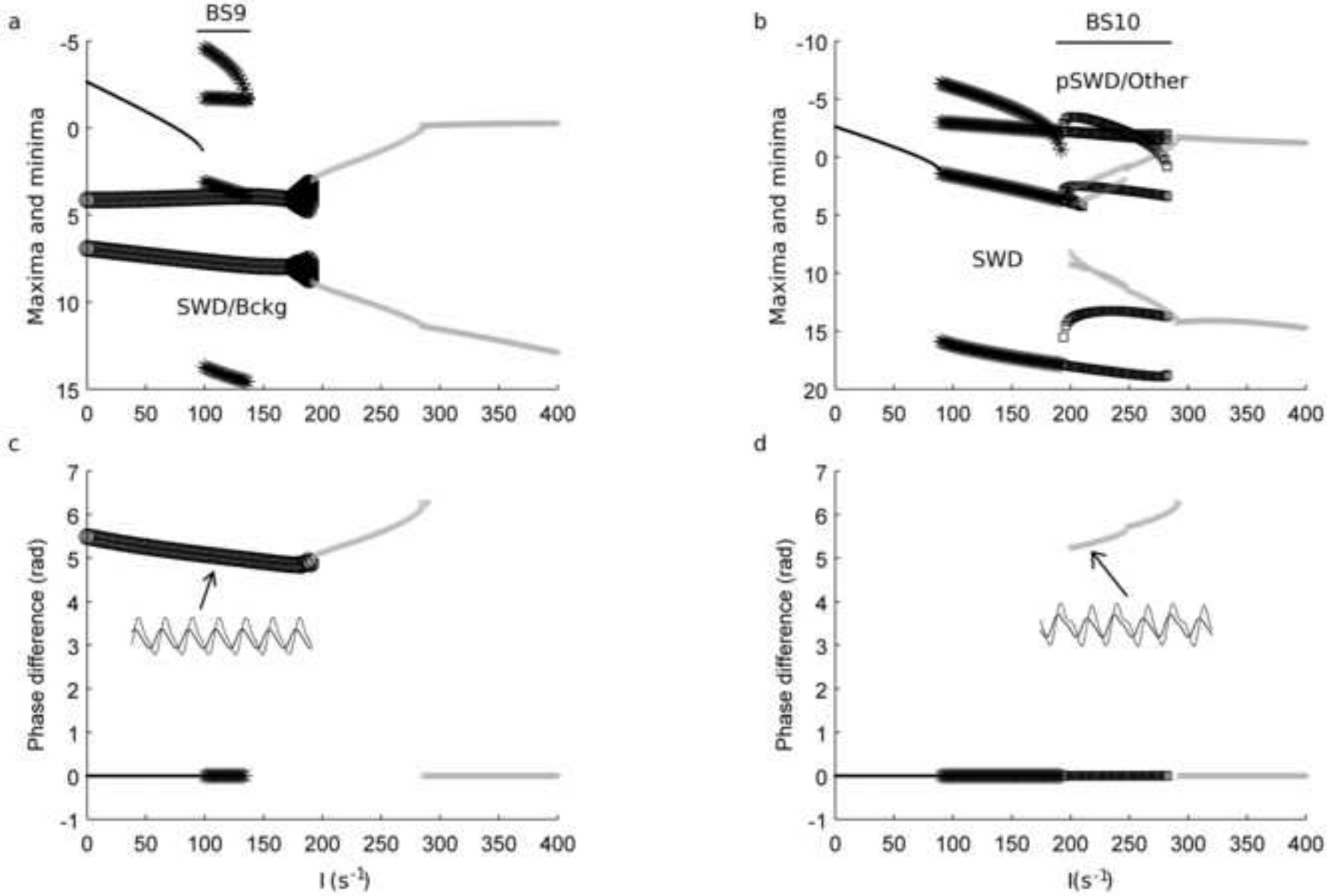

5. Figure

Click here to download high resolution image

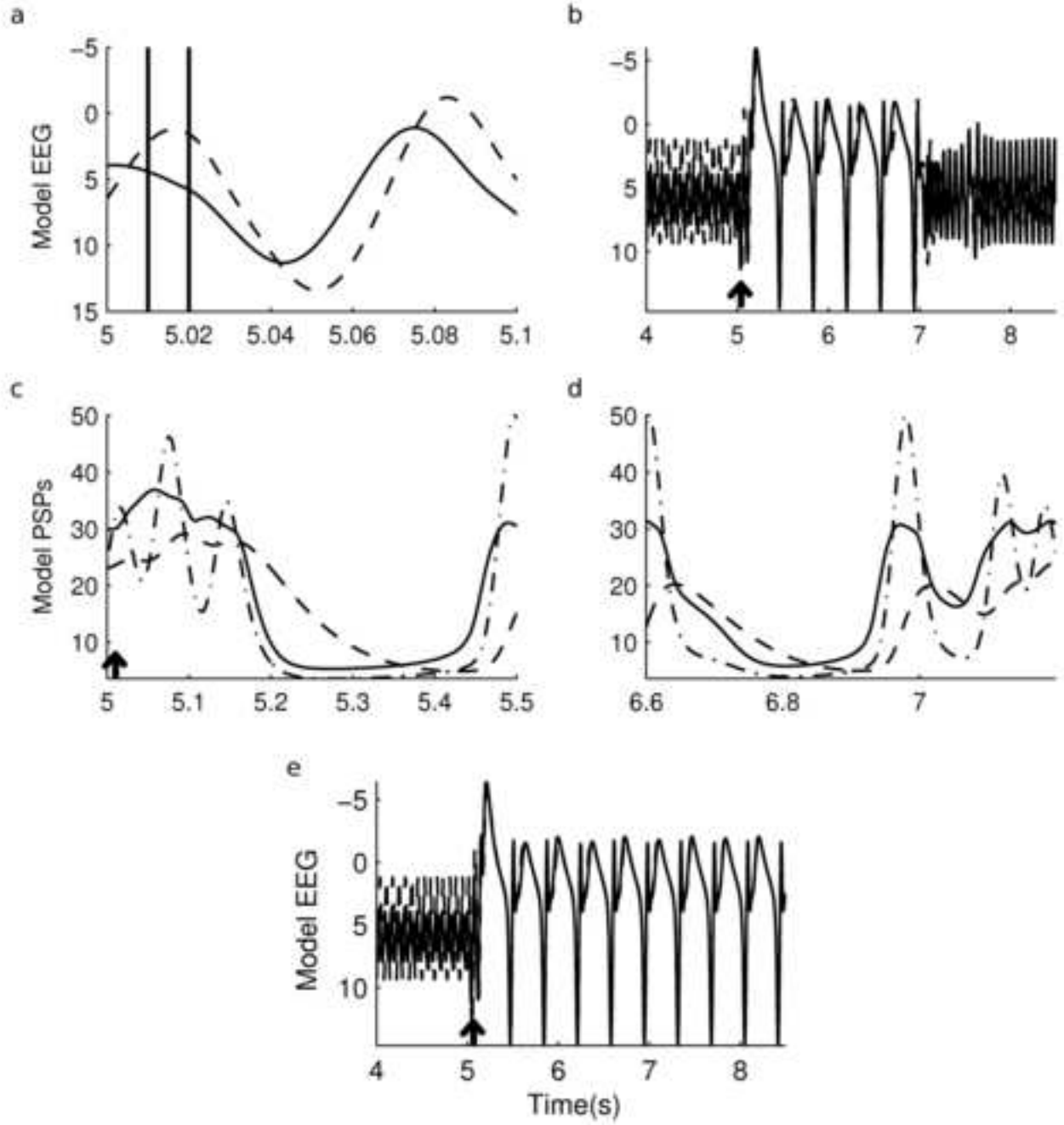

5. Figure

Click here to download high resolution image

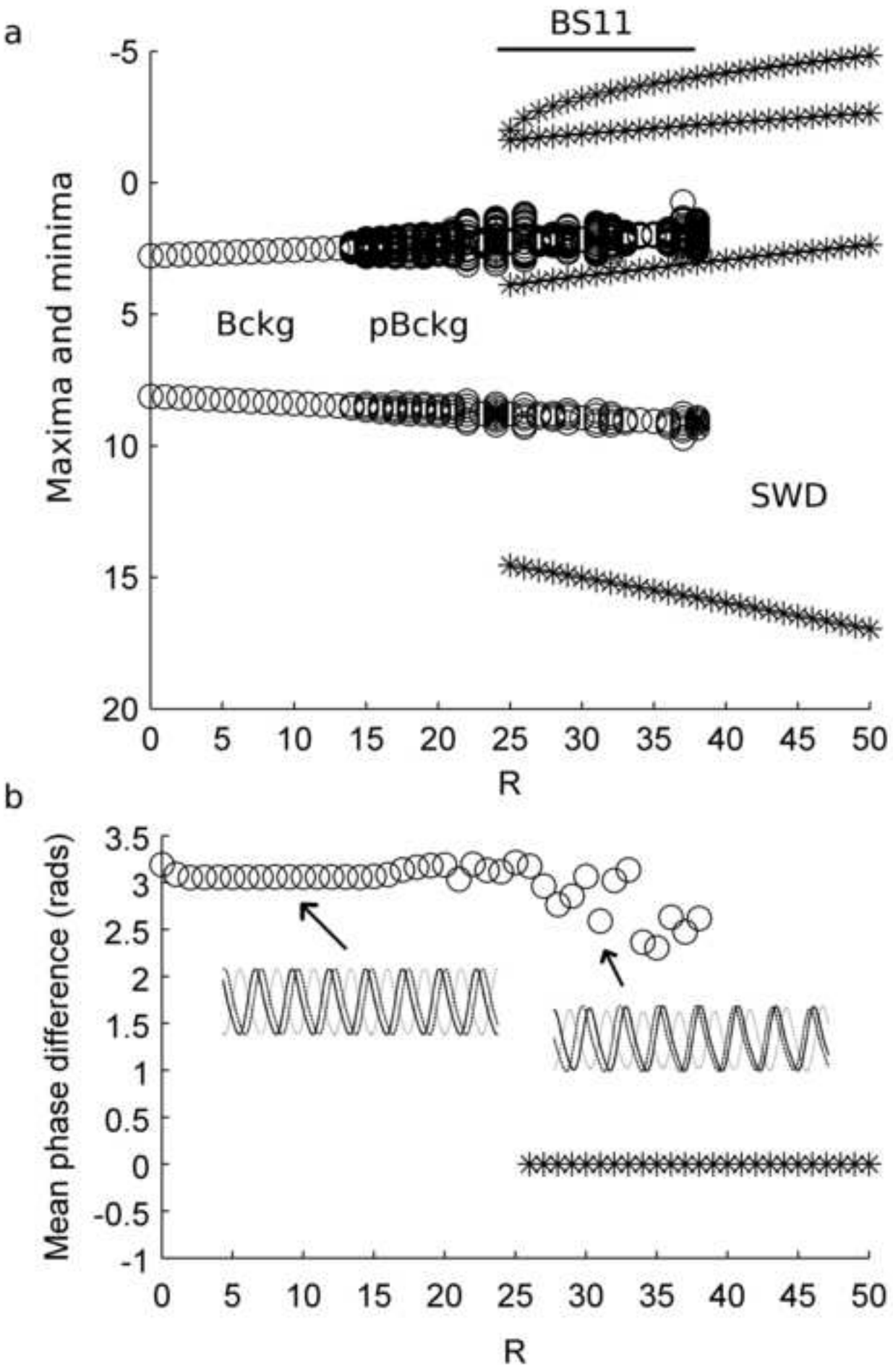

5. Figure

Click here to download high resolution image

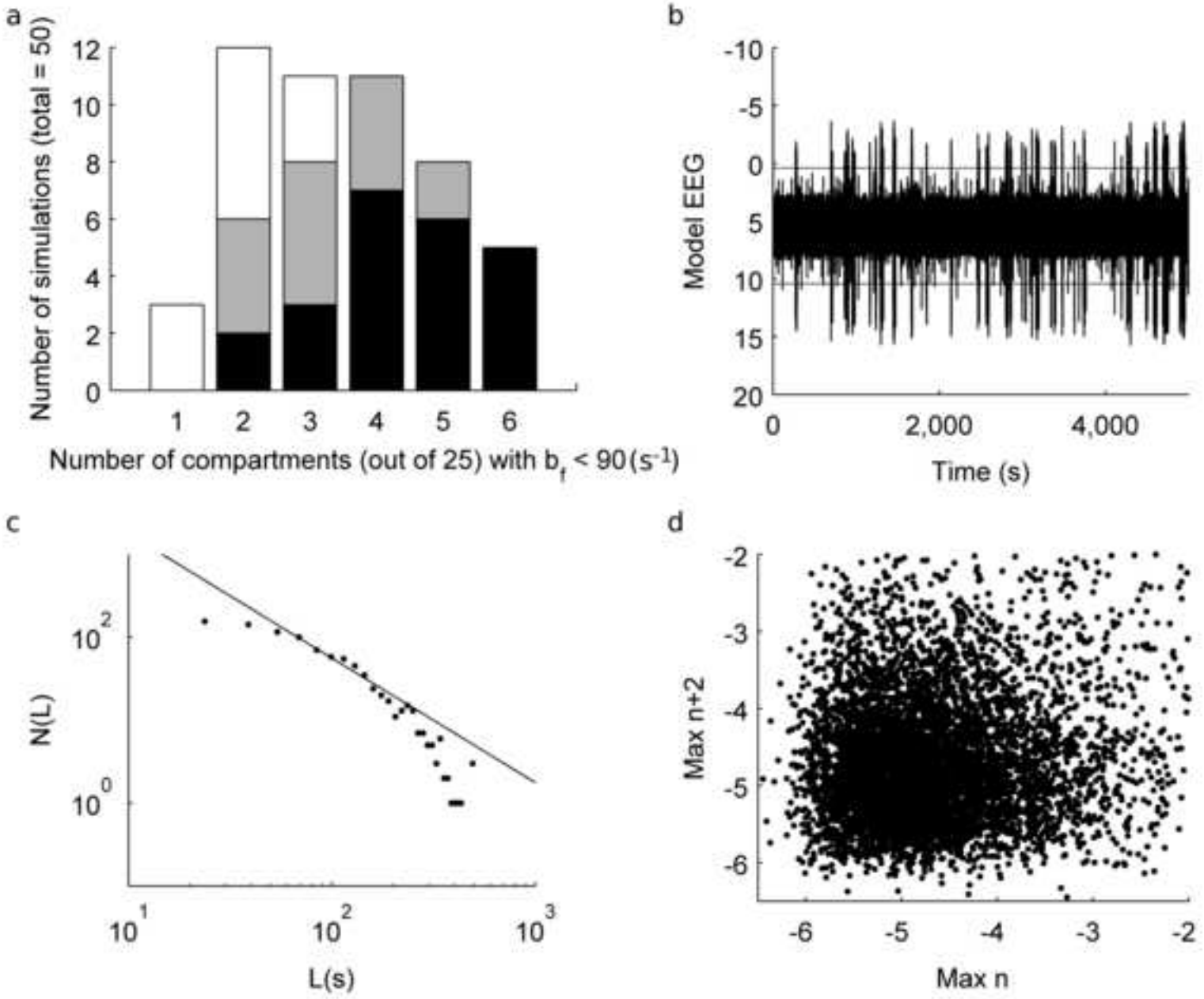

5. Figure

Click here to download high resolution image